A Reproduced Copy

OF

CASE FILE
COPY

Reproduced for NASA

by the

NASA Scientific and Technical Information Facility

FINAL SUMMARY REPORT

7511-70-R5

DESIGN AND DEVELOPMENT OF AN INTEGRAL BRUSHLESS DC TORQUER-ENCODER

CONTRACT NAS-8-24655

MARCH 1, 1970

PREPARED FOR

NATIONAL AERONAUTICS AND SPACE ADMINISTRATION

GEORGE C. MARSHALL SPACE FLIGHT CENTER

HUNTSVILLE
ALABAMA 35812

PREPARED BY:

SAUL MALKIEL
AVIONICS SYSTEMS

DEPARTMENT 7511

THE
BENDIX CORPORATION
NAVIGATION AND
CONTROL DIVISION
TETERBORO,
NEW JERSEY

Bendix Navigation & Control Division


RECEIVED
MAY 1970
NASA STI FACILITY
INPUT BRANCH

TABLE OF CONTENTS

1.0 INTRODUCTION

This final summary report describes the work done under contract NAS 8-24655. The original statement of work described a program in which an actual torquer-encoder would be constructed, tested, and shipped. This was later amended, limiting the requirement to a "recommended design".

Previous to this contract, NASA had obtained the development of a brushless torquer, suitable for use in torquing the output axis of the AMAB-3 Pendulous Integrating Gyroscopic Accelerometer (PIGA). This torquer and electronics was furnished on loan on this contract so that testing could make known the analog accuracy available from its magnetic structure. The present requirements, then, were to pinpoint error sources in the furnished torquer, determine how they could be reduced and make a recommended design for an integral brushless torquer-encoder, using the Hall resolver principle.

2.0 DISCUSSION OF HALL RESOLVERS

2.1 General Features

2.1.1 Operation

A Hall Resolver is here defined as a device operating by virtue of the Hall effect and having more accuracy than a Hall position sensor by definition. A Hall Resolver transduces shaft position into electrical analog signals. It does this by using the principle that a Hall generator gives an electrical signal output proportional to the product of the control current to the Hall generator times the magnetic flux normal to the Hall plate. If the control current is constant and the normal flux is arranged to vary sinusoidally with rotation, a sinusoidal output results. In the usual Hall resolver, a permanent magnet rotor, with sinusoidal magnetization along its circumference, is made to turn inside an iron return path. Interposed in the air gap are two Hall generators, spaced 90 electrical degrees apart.

The outputs of the two Hall generators are then the resolved shaft position, $\sin\theta$ and $\cos\theta$.

2.1.2 Application

A Hall resolver has the advantage of requiring no brushes or slip rings since its output is obtained from stationary Hall generators which are energized by the rotating permanent magnet. Another advantage is that the excitation to the resolver can be AC or DC.

When AC, output is modulated AC, much like that of a wound resolver, but unlike the wound resolver, the excitation may be DC in which case the outputs are slowly varying DC voltages which are constant at some fixed shaft position. For certain systems, this DC system may be preferable. Another advantage is that the output of a Hall resolver is proportional to the shaft position only and is independent of shaft velocity.

When a Hall position sensor is already present in a device, which is the case in Hall effect brushless motors, and where accurate shaft position readout is needed, in addition to that required for commutation, a logical extension of use of the position sensor is to modify it, thus constructing an accurate Hall resolver signal. In certain brushless motor designs, the Hall position sensor excitation is determined by the torque demand, and is therefore variable and not suitable as the Resolver-Digitizer excitation. In this case, there is ample unused circumference of air gap available for installation of separate Hall Generators. These added Hall generators, with their electronic circuits, form the Hall resolver. It is isolated electrically from the commutation position sensor. Its accuracy will be improved over the commutation position sensor by one of several methods. Reduction of analog error can logically begin with development of magnets with magnetization very closely sinusoidal. However, given an existing magnet, use of multiple Hall generators and other techniques to be discussed offer accuracy improvements. If the Hall resolver is subsequently

converted into digital form, then a digital shaft encoder has been built, without adding to the size of the brushless torquer in any way.

The number of poles must be the same in the motor and its position sensor. Thus using a two-pole motor, the resolver output will be single speed, where with a four-pole motor, a two-speed output results. With a two-speed or higher speed output, the output will be the same as if the resolver were driven at twice its speed thru a 2:1 step up gear train.

In the case of Hall resolvers not based upon a given motor, the number of poles may be selected. Since multispeeding increases the electrical degrees per mechanical degree over that with a two-pole design, all errors which depend upon the errors in electrical degrees will be reduced. The electrical component imperfections all given errors in electrical degrees, independent of number of poles. These electrical components include Hall generators, R-C networks and amplifiers. The electrical components therefore are favored by multi-speeding. A second type which is not improved is perpendicularity, that error due to lack of exact 90^{o} electrical spacing between Hall generators. However, it is possible by electrical adjustments to eliminate this error. A third type of error is one which may or may not be improved by multi-speeding. If multiple poles can be achieved without degrading the magnetization in terms of electrical degrees there will be an improvement. There may be diminishing returns as the electrical degree error may begin increasing at some number of poles.

2.2 Error Sources

This section lists the error sources of Hall resolvers and discusses the form which the error takes as seen in the analog output.

2.2.1 Non-Sinusoidal Magnetization Along The Circumference

The most significant component of this distortion is the third harmonic, and this will be the only component considered here.

The origin of the distortion lies in the inhomogeneity of permanent magnet material and in the difficulty of controlling the magnetization process closely.
The effect on the analog resolver error caused by a certain distortion percentage has been calculated in MT-14,620 (Sources of Hall Resolver Error). This error sensitivity is b_3 radians electrical error for a relative third harmonic of b_3, based on unity fundamental. This error shows up as a fourth electrical harmonic error.

2.2.2 Magnet Eccentricity

If the magnet geometric center does not coincide with its center of rotation, the magnet is said to run eccentric. This may be due to manufacturing tolerances.

The sensitivity of this effect is $\frac{e}{R} \sin \frac{90}{P}$ mechanical degrees where e is eccentricity in inches, R is the magnet radius, and P is the number of pole pairs.
This error shows up predominantly as a mechanical fundamental.

2.2.3 Hall Generator Resistive Null Temperature Coefficient

The misalignment between the output electrodes in a Hall generator gives an output voltage component which is not a product function as is the desired output, but is a constant amount independent of flux. It may be adjusted out using a standard nulling scheme with resistors. However as the Hall generator is put in different ambient temperatures, all portions of the crystal may not have the same characteristics and a resistive null may again appear. This temperature instability is a strong function of the method of construction used. Deposited film devices have high useful output but are more prone to this temperature shift than is the more expensive slab-type which is made by polishing an ingot to the required thickness. The latter have less output but their increased stability gives an improvement in the ratio of signal to null shift. Against this advantage must be weighed the much higher price and their relative fragility.

In MT-14,620, the sensitivity to resistive null was shown to be b_o radians electrical degrees where b_o is the ratio of null voltage to peak Hall voltage. Its form is that of an electrical fundamental.

2.2.4 Non-Linear Response Of Hall Generator To Flux

This appears to be a relatively insignificant error source. There are two reasons for this. The first is that the main non-linearity is a slight saturation effect at very high flux levels. The normal flux levels do not reach very high levels, minimizing this effect.

The second reason is that a flattening type of distortion goes over into the analog error but minimized, because the accuracy at these points is due almost completely to the accuracy of the other channel which is at or near zero.

2.2.5 Gain Unbalance Error

Gain unbalance between sine and cosine channels gives analog error. At calibration, the amplifiers will be adjusted to balance the channel gains. The individual Hall constant temperature coefficients may not track each other exactly giving an error with temperature. MT-14,620 shows that the sensitivity is $\frac{k-1}{2}$ radians electrical degrees error where k is the ratio of the two channel gains. The form is of a second harmonic electrical error phased such that its zero points occur at zeros of both the sine and cosine outputs.

2.2.6 Non-Perpendicular Placement Error

The source of error is the inability to space the two Hall generators at exactly 90^{o} to each other. It may arise due to assembly tolerances or, more likely, due to the inexact location of the active area of Hall generators with respect to their substrates. The calculated sensitivity is $\frac{\alpha}{2}$ radians mechanical error, where α is the amount the spacing differs from 90^{o}. Note that this error is in mechanical degrees and is independent of number of pole pairs. The form is second electrical harmonic, in quadrative to that of 2.2.5 above.

2.2.7 Pole-To-Pole Variations

This is similar to 2.2.1 but is specifically by definition only the distortion which varies pole-to-pole. Processes which improve the error of per 2.2.1 should also be helpful here.

2.3 Error Reduction Means

This section deals with means to improve Hall Resolver accuracy and discusses ways to reduce certain types of errors.

2.3.1 Multiple Hall Sensors

2.3.1.1 Reduction Of Error Induced By Third Harmonic Flux

Probably the most significant area for improvement in accuracy lies in elimination of third harmonic flux error. A method has been devised to reduce the coupling of third harmonic flux to the Hall generators. It is based on a principle very similar to that used in AC generator design to reject harmonics of a magnetomotive wave. In generators, the stator coil pitch can be chosen to be 360 degrees at third harmonic frequency. In this case, the third harmonic has been "pitched out". In an analogous way, if a Hall generator is replaced by two others located 30 degrees to either side of the replaced one, and the two Hall generator outputs summed, the output theoretically contains no component due to the third harmonic flux. The fundamental and fifth harmonic outputs are increased by a factor of $\sqrt{3} = 1.732$.

In MT-14,621 (Multiple Hall Generators For Hall Resolvers) the principle is discussed in more detail and a circuit is shown which performs the summing of Hall signals. The principle may be extended to fifth harmonic cancellation using 36 degree spacing. In this case there would be no improvement in the third harmonic. To generalize, two Hall generators can "pitch out" one harmonic and its multiples, depending upon the spacing used but the third harmonic is the most important error contributor for practical systems. The amplifier circuit uses an integrated circuit amplifier connected as a summing differential amplifier with single-ended output.

2.3.1.2 Reduction of Eccentricity Error

If two Hall generators, spaced 180 degrees mechanical are summed to form each channel output, and outputs summed with one reversed in sense the effect of eccentricity will be cancelled, theoretically completely. Multiple sensors may be required to reduce the error as described in 2.3.1.1 above. In a multi-pole unit, after the location of the first generator of the pair used in harmonic "pitching out" the second unit can go in any of n different locations where n=no. of poles and still have 60 degrees electrical spacing. One of these will be closest to also being 180 degrees mechanically spaced with the first. Thus, a large measure of rejection of eccentricity will be obtained, as a bonus for units with 4 poles or more.

With a two pole magnet, a 120 degree spacing is used. Figure 2.3.1.2-1 shows the vector diagram of the eccentricity. Since the error occurs once each mechanical cycle it may be represented by a vector rotating once per revolution. The amplitude of the sum of two vectors at 120^{o} is the same as the original vectors. With four poles, however, the sum is .518, and with 6 poles, the sum is 0.26. Thus, for multispeed units, there is an appreciable improvement factor.

2.3.1.3 Ability To Adjust Out Perpendicularity, Electrically

A third advantage of multiple sensors is that the effective axis of a pair with 60 degree spacing may be rotated slightly by favoring one of the pair by making its amplifier gain slightly greater. This may be done at calibration to remove the perpendicularity error.

2.3.1.4 Averaging Out Pole-To-Pole Variations

Since multiple Hall generators see different portions of the magnet at any given time there will be an averaging effect which will tend to reduce the effect of pole-to-pole variations of the magnet. The summed Hall outputs will therefore contain less signal due to pole-to-pole variations.

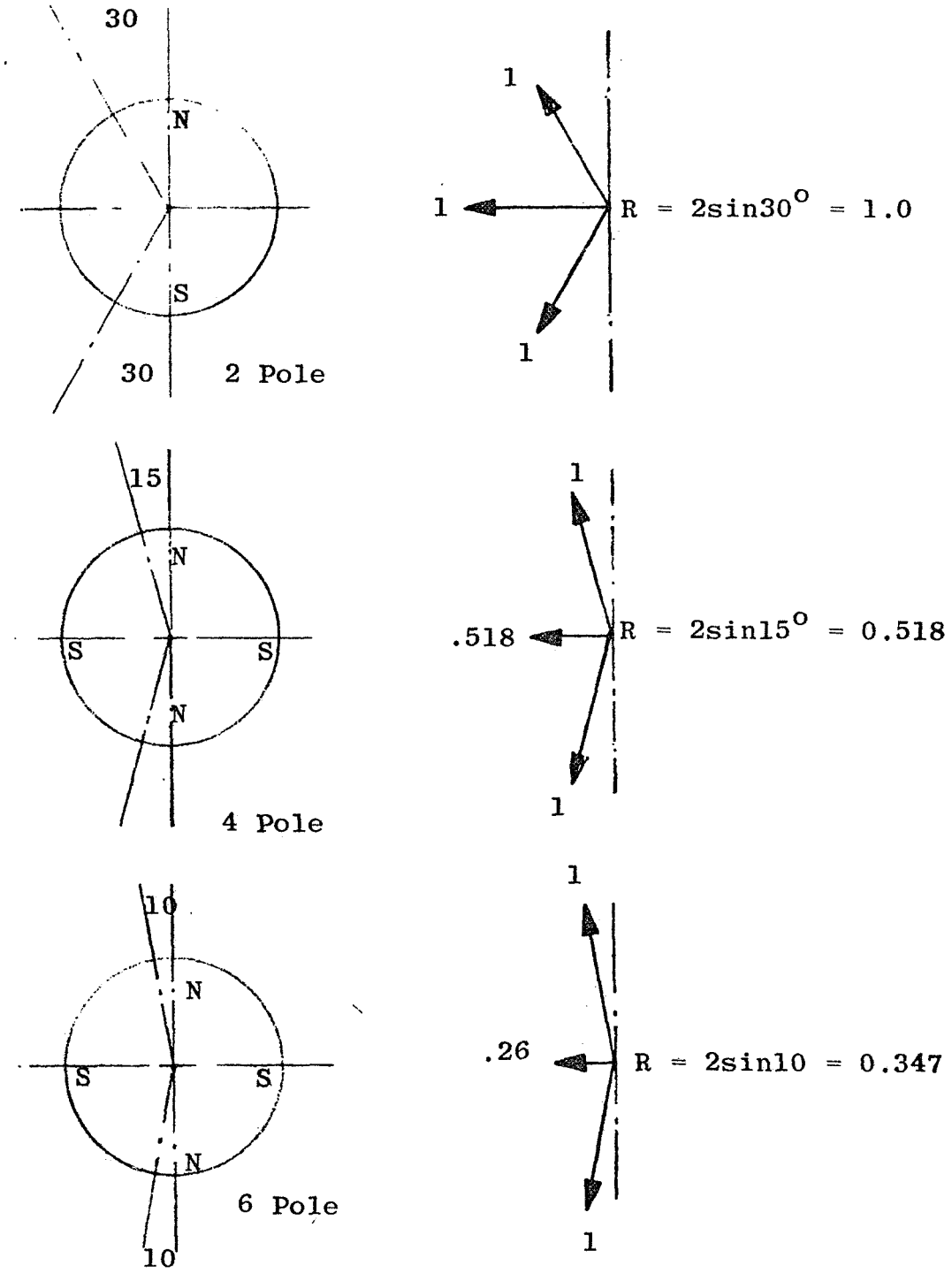

Figure 2.3.1.2-1

2.3.2 Use of Series Circuit For Hall Excitation

When the Hall generators have their control circuits in series, a change in resistance of any generator effects the current through all the units, equally. In this case only a change in resolver gain occurs but no analog error. The two main causes of resistance change are change in resistance as a function of flux (magnetoresistance effect) and temperature coefficient of resistivity. With a series connection, there is more common-mode voltage at the inputs to the Hall amplifiers but modern microcircuits have sufficient common-mode rejection to give no accuracy problem.

2.3.3 The reduction of errors due to imperfect tracking of the hall generators with temperature depends upon availability of matched sets of devices. At least on e manufacturer (Siemans) offers matching services thru their U.S. distributor. The important matching parameters here are:

1) Tracking of the temperature coefficients of the Hall voltage.

2) Low resistive nulls, and perhaps also some tracking of nulls with temperature.

Verification of accuracy versus temperature would require laboratory testing of resolvers.

2.3.4 Sinusoidal Rotor Magnetic Flux

It is obvious that the more sinusoidal the air gap flux distribution, the more sinusoidal will be the Hall generator output. Various magnet materials and constructions as limited by the particular geometry of an assembly, could be fabricated and sophisticated magnet changing and treating techniques applied to obtain the best sinusoidal flux pattern.

The problems of manufacturing a rotor with sinusoidal flux distribution include non-homogeneous materials, tolerance variations in magnetic properties from magnet to magnet and machining tolerance variations causing pole spacing and/or pole tilting errors.

To determine which offers the best error-reducing trade-off the relative merits of various multipole magnets as follows could be investigated.

1. Integral magnet - This is a single cost or sintered magnet which is machined to size and used without pole pieces. Machining tolerance and magnetic property tolerance errors can be minimized and mechanical construction is relatively simple. However, magnet inhomogeneities and difficulties in charging, treating and adjusting for sinusoidal flux distribution are limiting factors.

2. Circumferential enclosed magnet assembly- This consists of individual bar magnets circumferentially located in a precisely machined magnetic pole structure. It is a relatively complex mechanical

structure with accuracies limited by machining tolerance errors. However, the assembly permits matching of individual magnets to minimize errors due to magnet inhomogeneities and magnetic property tolerances. The completed structure can also be more easily charged, treated and adjusted to minimize flux distribution errors. This assembly is also most effectively keepered for easy handling.

3. Radial exposed magnet assembly - This consists of individual bar magnets radially located on a magnetic hub. Its characteristics are much like the circumferential assembly described above except that charging, treating, adjusting the flux pattern and keepering is more difficult.

As indicated, magnet charging and treating techniques will have a significant effect on flux distribution and on magnet stability. The effects of various charging and treating fixtures, keepering requirements and handling procedures would be studied to achieve an optimum sinusoidal flux pattern.

3.0 EXPERIMENTAL EVALUATION OF FURNISHED TORQUER

The purpose of this evaluation was to determine analog error of the furnished torquer, first by obtaining an error curve by test, then by analyzing it into Fourier components, and then finally, using known cause and effect relationships between an error source and the resultant Fourier component of the error curve, pinpoint the error source and its amplitude. A check of the validity of the error curve was made by doing an additional test of the sine deviation. In this test rather than checking the ratio of the two resolver signals with a resolver bridge, as is done to get analog error, each output is tested individually for conformity with ideal sine and cosine waves. The result of this test confirmed the previous test.

3.1 Testing

MT-14,609, (Hall Resolver Test Report) describes, in detail, the test procedure used and the results. The two existing Hall Generators were used and were driven by the Hall drivers and their outputs were amplified by the summing amplifiers of the Brushless Torquer electronics. A 1000 Hz signal was used to drive the Hall generators to about 25 ma peak. Slight modifications were made to lower the gain of the summing amplifiers to keep their outputs in the linear range. No DC servo error signal was present in this testing.

The unit was indexed in 4 degree steps and the output error determined with a resolver bridge. The error was then graphed on p10 of MT-14,609. The twelfth

harmonic stands out, but visually it is not possible to definitely identify any other harmonics.

3.2 Computer Done Fourier Analysis

This error curve was analyzed by digital computer and the computer printout is on page 15 of the MT.The result is quoted here in Table I, for amplitudes above 0.1 degree electrical.

TABLE I

Space Harmonic Number	Elec. Degrees	Mech. Degrees	Phase	Source
12	2.95	0.98	-170^{o}	3rd elec. harmonic flux
1	0.83	0.28	-165^{o}	eccentricity
6	0.46	0.15	0.0	gain unbalance
	0.74	0.25	90.0	non-perpen. placement
5	0.70	0.23	-75^{o}	Due largely to magnet pole-to-pole variations
4	0.28	0.09	-37^{o}	
8	0.28	0.09	-139^{o}	
7	0.22	0.07	-64^{o}	
9	0.19	0.06	-158^{o}	
3	0.18	0.06	80^{o}	Uncompensated Hall resistive Nulls

Since this is a 3 speed unit (6 poles), the electrical fundamental error is the 3rd space harmonic.

3.3 Error Amplitudes And Sources

A mathematical analysis was made which related an error source within the resolver to a particular Fourier component of the analog error and this was reported in MT-14,620 (Sources of Hall Resolver Errors). The last column of Table I lists these sources.

The largest component is due to the twelfth space harmonic. The cause is 3rd electrical harmonic magnet flux. The magnitude is 2.95^{o} electrical or 0.98^{o} shaft.

The second largest component is the first harmonic (fundamental). Part of this may be due to the magnet running about a center other than its geometric center (eccentricity). Another contribution may be due to misalignment between the dividing lead test shaft and the resolver shaft. It is not known the relative contributions of each. The total magnitude is 0.83^{o} electrical or 0.28^{o} shaft.

The third largest component is the quadrature component of the sixth harmonic. This is due to error in perpendicularity between the two Hall generators. The magnitude is 0.74^{o} electrical or 0.25^{o} shaft.

The next component is the in-phase component of the sixth harmonic. This is due to unbalance between sine and cosine outputs. The magnitude is 0.46^{o} electrical or 0.15^{o} shaft.

Next there is a group containing the 5th, 4th, 8th, 7th and 9th harmonics. These are due to pole-to-pole variations in the magnet.

Finally there is the 3rd harmonic. This component is due to uncompensated Hall generator resistive nulls. Its magnitude is 0.18^{o} electrical or 0.06^{o} shaft.

3.4 Error Remaining With Use Of Error Cancellation Schemes

If the previously considered error reduction schemes are utilized, and they accomplish their desired result, perfectly, the errors due to the space harmonics of numbers 12, 1, 6 and 3 will be zero. Referring to Table I, the remaining significant harmonics are of numbers 5, 4, 8, 7 and 9. These last are due largely to variations in the strength and placement of the six poles. Combining these last 5 components in RSS fashion, the resultant is 0.275 degrees mechanical. The peak present error may be derived from page 2 of MT-14,609, by taking the total error spread (+7.13 to -2.17) or 9.30 peak-peak, dividing by two to obtain the peak, and dividing by three to get the mechanical degrees. This calculation gives 1.55 degrees mechanical. The ability to reduce this to 0.275 degrees, without changing the magnet, is significant. Of course in practice, the full improvement would not be obtained, but it could be approached.

4.0 RECOMMENDED DESIGN

The basic features in the recommended design are the use of multiple Hall sensors with each channel pair spaced at 60 fundamental electrical degrees apart, and with the 4 Hall generators driven in series. They are Siemens type SV210, made of vapor-deposited InAs. Provision is made, in the Hall output amplifiers, for electrically compensating for perpendicularity error. The generators are spaced mechanically to partially remove eccentricity error.

There are various methods of resolver-to-digital conversion. For this application the phase-multiplication method does not offer any advantage and is relatively complex. Methods using DC excitation of the resolver with digitally controlled generation of sineθ and cosθ are also complex. Of the two schemes using carrier excitation, the first excites the two channels in quadrature. The networks providing the 90^{o} phase difference is subject to change due to capacitor variations with temperature. The second method was common excitation but has two RC networks on the resolver outputs. In this case the error depends only upon the degree to which the two capacitors do not track, perfect tracking giving no error. The capacitor problem then is not severe. This last method is one with which Navigation and Control Division has ample experience, having built and delivered such systems.

The spacing between the multiple Hall generators of one channel is 160^{o} mechanical. It was shown in section 2.3.1.2 that this spacing, for a 6 pole rotor reduces the eccentricity error down to 0.347 of that picked up by a single generator. Figure 4.0-1 shows a sketch of the non-magnetic retainer ring for the four Hall operators, to fit inside the brushless torquer as a replacement for the two-generator retainer ring.

In DWG 1976682 is shown the block diagram of the recommended design. Beginning at the position sensor, the four Hall generators are driven by the Hall driver, in series. The two existing generators for the torquer are also shown. There is one Hall output amplifier which sums the signals of the two Hall generators forming the $\sin\theta$ output, and a similar amplifier forming the $\cos\theta$ output. These two variable amplitude signals go to the resolver-to-phase converter. This consists of two RC networks, the outputs of which are two constant amplitude signals. The phase of one output leads and the other lags with a certain directionof shaft rotation, such that a phase difference between the two signals exists which is double that for a single R-C network. The phase meter following detects the phase difference, by measuring the time difference between the zero crossings of the two waves. The phase meter output is a logic signal, whose pulse width is proportional to shaft rotation angle. The output has a 6 fold redundancy. That is, in one sixth of the total rotation, i.e. in 60^{o} shaft rotation, the duty cycle of the pulse width

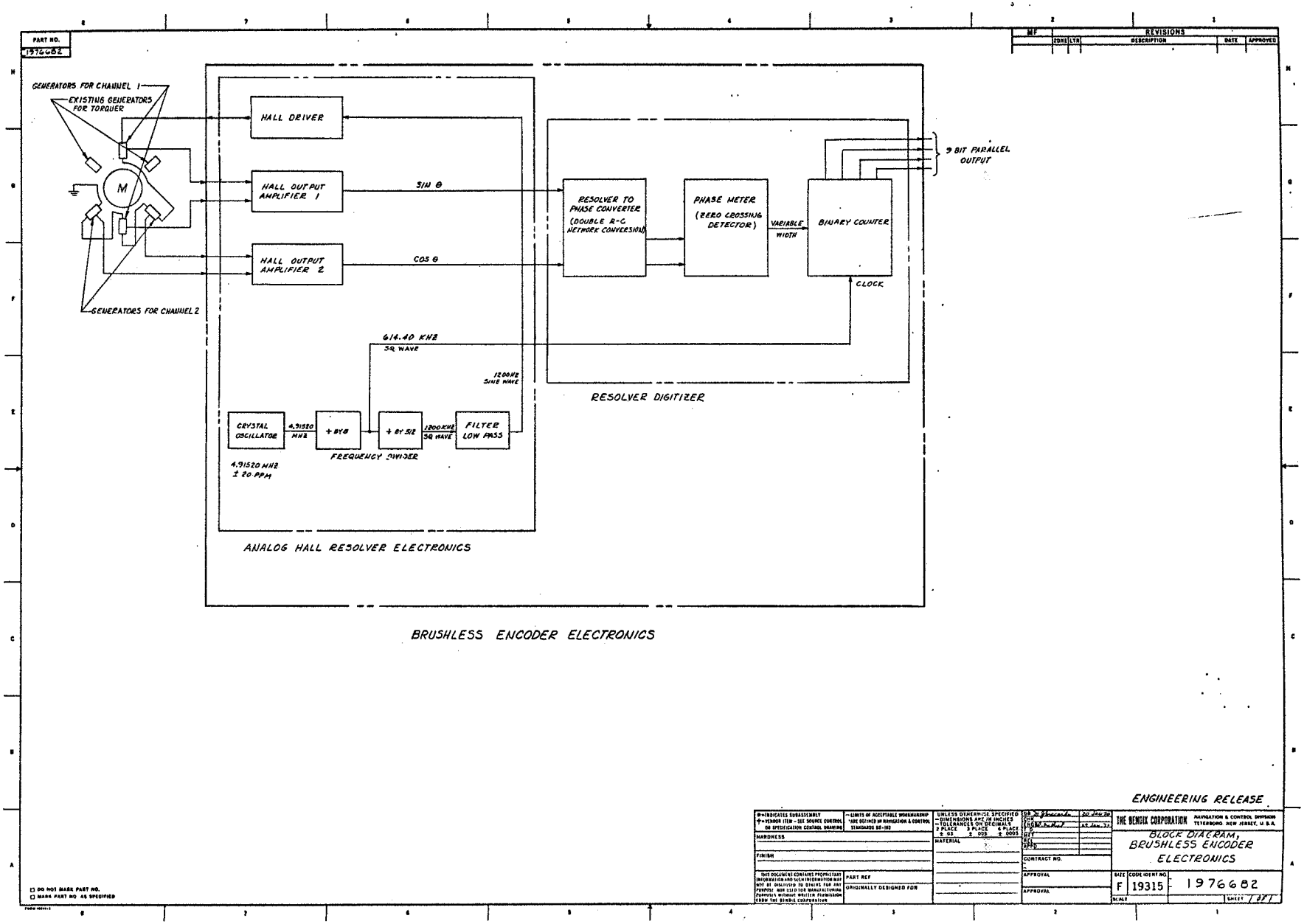
PART NO. 1976682
REVISIONS
MF ZONE LTR DESCRIPTION DATE APPROVED
GENERATORS FOR CHANNEL 1
EXISTING GENERATORS FOR TORQUER
M
GENERATORS FOR CHANNEL 2
HALL DRIVER
HALL OUTPUT AMPLIFIER 1
HALL OUTPUT AMPLIFIER 2
SIN θ
COS θ
RESOLVER TO PHASE CONVERTER (DOUBLE R-C NETWORK CONVERSION)
PHASE METER (ZERO CROSSING DETECTOR)
VARIABLE WIDTH
BINARY COUNTER
9 BIT PARALLEL OUTPUT
CLOCK
RESOLVER DIGITIZER
614.40 KHZ SQ WAVE
1200HZ SINE WAVE
CRYSTAL OSCILLATOR
4.91520 MHZ
÷ BY 8
÷ BY 512
1200 KHZ SQ WAVE
FILTER LOW PASS
FREQUENCY DIVIDER
4.91520 MHZ ± 20 PPM
ANALOG HALL RESOLVER ELECTRONICS
BRUSHLESS ENCODER ELECTRONICS
ENGINEERING RELEASE
THE BENDIX CORPORATION NAVIGATION & CONTROL DIVISION TETERBORO, NEW JERSEY, U.S.A.
BLOCK DIAGRAM, BRUSHLESS ENCODER ELECTRONICS
SIZE F
CODE IDENT NO. 19315
1976682
SHEET 1 OF 1
DO NOT MARK PART NO.
MARK PART NO AS SPECIFIED

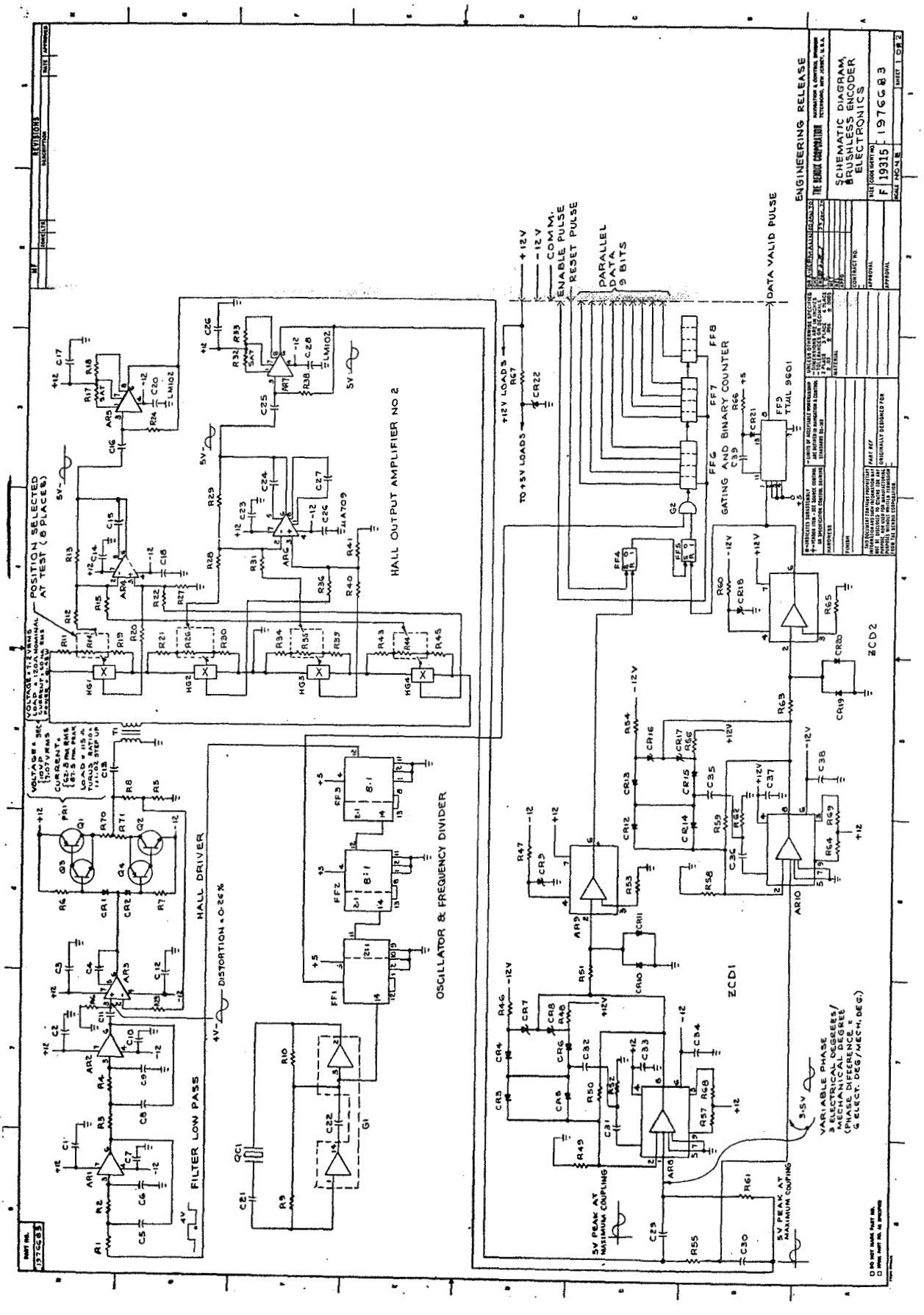
ENGINEERING RELEASE
SCHEMATIC DIAGRAM, BRUSHLESS ENCODER ELECTRONICS
F 19315
1976683
HALL OUTPUT AMPLIFIER NO 2
HALL DRIVER
FILTER LOW PASS
OSCILLATOR & FREQUENCY DIVIDER
GATING AND BINARY COUNTER
DATA VALID PULSE
PARALLEL DATA 9 BITS
ENABLE PULSE
RESET PULSE
COMM.
+12 V
-12 V
+12 V LOADS
TO +5V LOADS
POSITION SELECTED AT TEST (6 PLACES)
VARIABLE PHASE
ZCD1
ZCD2

70-631

23

PART NO. 1976683

REVISIONS					
MF	ZONE	LTR	DESCRIPTION	DATE	APPROVED

SCHEM SYMBOL	DESCRIPTION
RESISTORS	
R1	0.1M
R2	0.1M
R3	0.1M
R4	0.1M
R5	1K
R6	10K
R7	10K
R8	1500
R9	619
R10	619
R11	2K
R12	10K
R13	500K
R14	SAT 0-10 Ω
R15	10K
R16	100K
R17	SAT 100-1000Ω
R18	500
R19	SAT 1500-2500
R20	10K
R21	10K
R22	10K
R23	100K
R24	.1M
R25	SAT 50K-150K
R26	SAT 0-10 Ω
R27	500K
R28	10K
R29	500K
R30	SAT 1500-2500
R31	10K
R32	SAT 100-1000Ω
R33	500
R34	2K
R35	SAT 0-10
R36	10K
R37	SAT 50K-150K
R38	.1M
R39	SAT 1500-2500Ω
R40	10K
R41	500K
R42	150Ω
R43	2K
R44	SAT 0-10
R45	SAT 1500-2500
R46	221K
R47	150Ω
R48	221K
R49	2K
R50	200K
R51	5100
R52	470

SCHEM SYMBOL	DESCRIPTION
RESISTORS	
R53	5100
R54	221K
R55	WW NON INDUCTIVE 15,504 K
R56	221K
R57	100K
R58	2K
R59	200K
R60	1500
R61	WW NON INDUCTIVE 15,504 K
R62	470
R63	5100
R64	100K
R65	5100
R66	10K
R67	150Ω 1W
R68	
R69	
R70	
R71	
CAPACITORS	
C1	0.1 μf
C2	0.1 μf
C3	0.1 μf
C4	30 pf
C5	0.00331
C6	.00053
C7	0.1
C8	0.00331
C9	.00053
C10	0.1 μf
C11	0.47/100V
C12	0.1 μf
C13	NON POLAR 10 μf 10V
C14	0.1 μfd
C15	30 pf
C16	0.1 μf
C17	0.1 μfd
C18	0.1 μf
C19	0.1 μf
C20	0.1 μf
C21	SAT 20-35 pf
C22	.01/200
C23	0.1 μf
C24	30 pf
C25	0.1 μf
C26	0.1 μf
C27	100 pf
C28	0.1 μf
C29	BALCO PTHM 0.0068 μf

SCHEM SYMBOL	DESCRIPTION
CAPACITORS	
C30	BALCO PTHM 0.0068 μf
C31	500 pf
C32	220 pf
C33	0.1 μf
C34	0.1 μf
C35	220 pf
C36	500 pf
C37	0.1 μf
C38	
C39	
C40	
C41	
DIODES	
CR1	SIN914
CR2	SIN914
CR3	SIN914
CR4	SIN914
CR5	SIN914
CR6	SIN914
CR7	SIN742
CR8	SIN742
CR9	SIN743
CR10	SIN914
CR11	SIN914
CR12	SIN914
CR13	SIN914
CR14	SIN914
CR15	SIN914
CR16	SIN742
CR17	SIN742
CR18	SIN743
CR19	SIN914
CR20	SIN914
CR21	SIN914
CR22	SIN761
TRANSISTORS	
Q1	2N2907
Q2	2N2222
Q3	2N2222
Q4	2N2907

SCHEM SYMBOL	DESCRIPTION
GATES	
G1	SN5404
G2	SN5400
FLIP FLOP	
FF1	SN5493
FF2	SN54L93
FF3	SN54L93
FF4	FC9950
FF5	FC9850
FF6	SN5490
FF7	SN5490
FF8	SN5490
FF9	FCTTUL 9601
LINEAR INTERATED CIRCUIT	
AR1	LM102
AR2	LM102
AR3	LM101
AR4	LM101
AR5	LM102
AR6	LM101
AR7	LM102
AR8	PHILBRICK Q25AH
AR9	μA710
AR10	PHILBRICK Q25AH
AR11	μA710
QUARTZ CRYSTAL	
QC1	PIONEER CENTRAL 1617525
GATES	
G1	SN5404
G2	SN5400

NOTE:
ALL RESISTORS ARE RN55C
EXCEPT WHERE OTHERWISE SPECIFIED.

☐ DO NOT MARK PART NO.
☐ MARK PART NO. AS SPECIFIED

⊕=INDICATES SUBASSEMBLY ✣=VENDOR ITEM - SEE SOURCE CONTROL OR SPECIFICATION CONTROL DRAWING	— LIMITS OF ACCEPTABLE WORKMANSHIP ARE DESCRIBED IN NAVIGATION & CONTROL STANDARDS 85-193	UNLESS OTHERWISE SPECIFIED — DIMENSIONS ARE IN INCHES — TOLERANCES ON DECIMALS 2 PLACE ± .03 3 PLACE ± .005 2 PLACE ± .005	DR ALMEIDA 2-MAR-76	THE BENDIX CORPORATION	NAVIGATION & CONTROL DIVISION TETERBORO, NEW JERSEY, U.S.A.
HARDNESS		MATERIAL	CHK	SCHEMATIC DIAGRAM BRUSHLESS ENCODER ELECTRONICS	
FINISH			ENG		
THIS DOCUMENT CONTAINS PROPRIETARY INFORMATION AND SUCH INFORMATION MAY NOT BE DISCLOSED TO OTHERS FOR ANY PURPOSE NOR USED FOR MANUFACTURING PURPOSES WITHOUT WRITTEN PERMISSION FROM THE BENDIX CORPORATION.	PART REF	CONTRACT NO.	MFG		
	ORIGINALLY DESIGNED FOR	APPROVAL	APPROVAL	SIZE F	CODE IDENT NO. 19315
				SCALE	SHEET 2

1976683

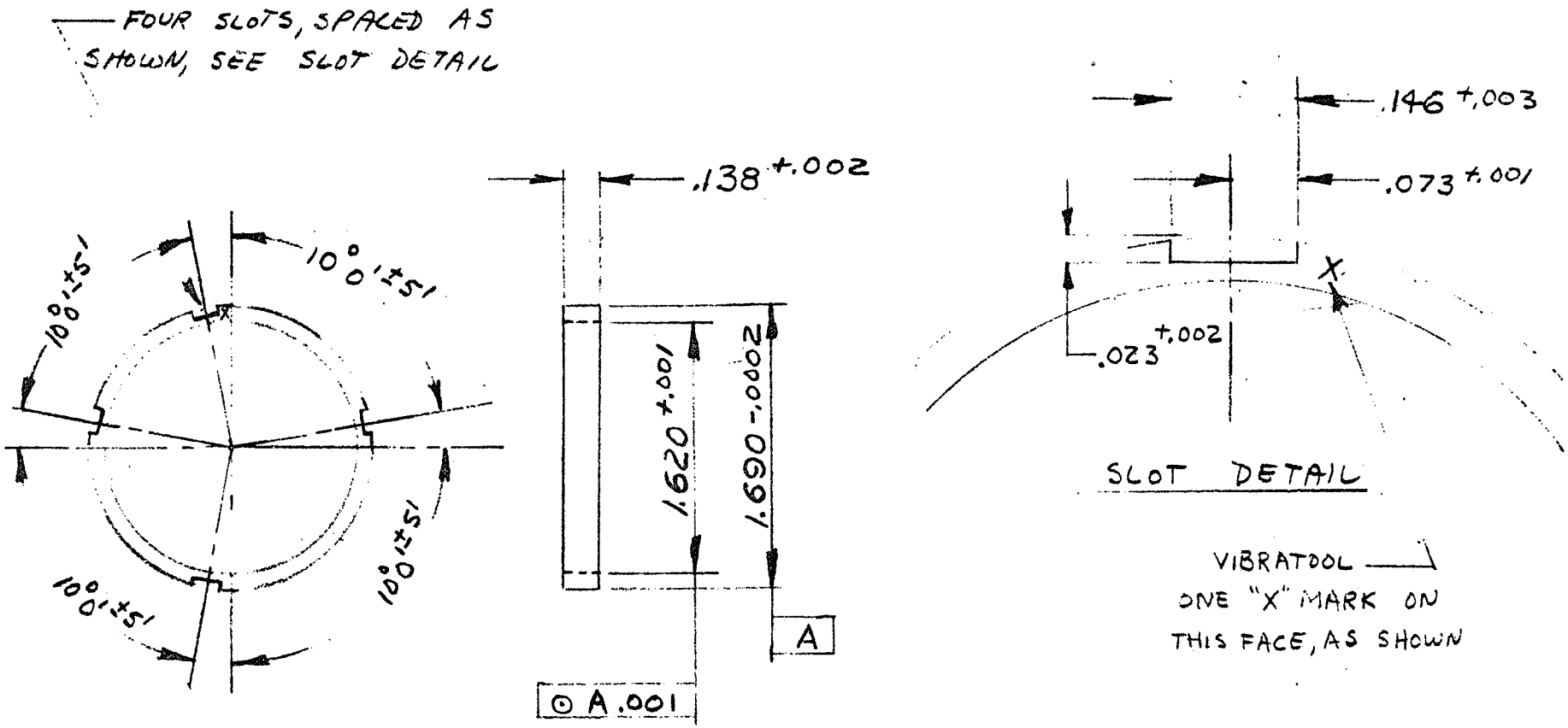

FIGURE 4.0-1

SPACER RING
SKETCH # SKJH 010570-3
MAT'L: BRASS

reaches 100%. The six-fold redundancy is made up of the factor 3 due to the 3 pole pairs and a doubling due to the double R-C networks used.

The variable width becomes a gating signal to the binary counter. When this signal enables a gate, the clock pulses enter the counter stages and the count accumulates. At the moment when the gating signal goes low, it will trigger a circuit which will put out a data validity pulse, indicating that the number in the register is valid and available, to be transferred out, in parallel.

The timing circuits generate the carrier and clock frequencies starting with a crystal oscillator and dividing down. The 1200Hz square wave is filtered to sine wave in the low pass filter before going to the Hall driver.

4.1 Selection Of Clock Frequency

The frequency of the AC carrier applied to the two Hall generators is chosen as 1200Hz. This frequency is high enough such that the stable capacitors for the phase shifters in the resolver-to-phase portion of the encoder are of reasonable volume, and yet not high enough to cause a severe accuracy problem on the zero-crossing detectors, due to detector phase shift and stray circuit capacitances.

The double R-C conversion method used together with the 3-pole-pair rotor makes each resolution step less by a factor of six than that for a 1-pole-pair rotor

used with a single R-C network conversion. Thus, if the ratio $\frac{\text{clock rate}}{\text{resolver excitation}} = n$, the resolution steps are $\frac{2\pi}{n(6)}$ mechanical radians.

It has been previously shown in 3.4 that error cancellation techniques could not reduce the error to below 0.275 degrees mechanical. The resolution step due to the digitizing should be below this, say 0.1 degrees. Letting the equation of the previous paragraph equal to $0.1 \times \frac{2\pi}{360}$, there results n=600. Since it is desired to choose an n which can be developed by a simple binary frequency divider, n will be chosen to be equal to $512(2^9)$, the nearest value of 2 raised to an integral power. The actual resolution element then comes out to be $\frac{360}{512} \times \frac{1}{6} = 0.117$ degrees mechanical. The clock frequency comes out to be 1200(512)=614.4kHz

4.2.2 Low Pass Filter

The low pass filter consists of two stages. Each stage is an active filter segment of the type shown in Fig. (4.2.2-1).

The transfer function for the filter segment is given by:

$$\frac{e_o}{e_i}(s) = \frac{1}{R_1 R_2 C_1 C_2 S^2 + (R_1+R_2)C_2 S + 1} = \frac{\omega_o^2}{S^2 + 2\delta\omega_o S + \omega_o^2}$$

where $w_o = \frac{1}{(R_1 R_2 C_1 C_2)^{1/2}}$

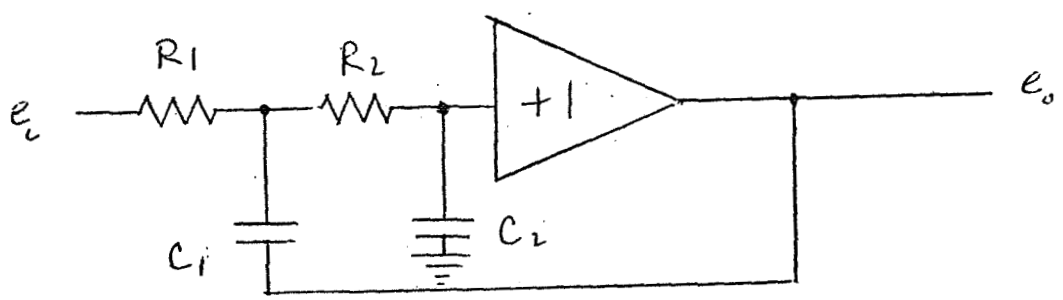

ACTIVE FILTER SEGMENT

FIGURE (4.2.2.-1)

$$\delta = \left(\frac{R_1 + R_2}{2}\right) \left(\frac{C_2}{R_1 R_2 C_1}\right)^{1/2}$$

R_1 and R_2 will be chosen to be 0.1 MΩ each. The filters will be tuned to 1200 Hz with a damping factor of 0.4, from which a gain will be realized at the operating frequency. Solving the above gives C_1 = 0.00331 ufd and C_2 = .00531 ufd.

The phase shift and amplitude ratio at ω_o is found from,

$$\frac{e_o}{e_i} = \frac{\omega_o^2}{S^2 + 2\delta\omega_o S + \omega_o^2}$$

$$S = j\omega_o$$

$$\frac{e_o}{e_i} = \frac{\omega_o^2}{\omega_o^2 + j^2\omega_o^2 + 2j\delta\omega_o^2} = \frac{\omega_o^2}{2j\delta\omega_o} = \frac{1}{2j\delta}$$

The phase shift is thus 90^o lag and the gain is 1.25.

The Fourier expansion of the square wave driving the active filters is

$$E = \frac{1}{\pi} E \left(\frac{\pi}{2} + \sin\omega t + \frac{1}{3}\sin 3\omega t + \ldots\right)$$

where E is the peak of the square wave voltage.

The third harmonic is the one requiring the most filtering. At the filter output it will be reduced to $\frac{1}{3} \times \frac{1}{9} \times \frac{1}{9} = .00412$. The fundamental will be increased by $(1.25)^2 = 1.56$. The third harmonic will thus be 0.002464 of the fundamental at the filter output, and the higher order components will be negligible in comparison.

The output of the two filters will be $\frac{2}{\pi} E (1.25)^2$. With E = 4.0V, the output is 3.98V peak.

The unity gain amplifiers are LM102 voltage followers.

4.2.4 Hall Driver Amplifier

The Hall driver amplifier is a power amplifier with a complementary symmetry output stage, driving into an output transformer which isolates the load from the transistors, allowing the center of the load to be grounded, and matches load impedance for highest efficiency. The circuit consists of a voltage amplifier driving the power amplifier, with heavy inverse feedback from the transformer primary back to the input, to insure low distortion. The voltage amplifier is a μA709, capacitor coupled to the filter. The power amplifier complementary transistors are diode biased to give a small idling current which prevents cross-over distortion. A portion of the output is fed back to the input such that a gain of 2.5 exists.

4.2.5 Hall Output Nulling Network

Each Hall network is bridged by a network of three series resistors to adjust out the resistive null. To null the top Hall generator for example, set R14=0 and adjust R19 so that the voltage at the right hand Hall output is equal to the voltage at the top of R19. Then connect the Hall output wire to the network and adjust R14 for best resistive null, that is the amplifier output is minimum in the absence of magnetic field. Similarly, adjust the three other generators.

4.2.6 Hall Output Signal Amplifiers

Each of the two channels consists of a μA709 voltage amplifier driving an LM102 voltage follower. The voltage amplifier has two inputs. One is the differential voltage corresponding to one Hall generator and the other is the second Hall voltage. The amplifier sums these two differential signals and amplifies them to the 5 volt level. Capacitor coupling is used to the buffer. The buffer is used to decouple any DC null voltage from the differential amplifier and to give a convenient null adjustment point.

4.2.6.1 Null Adjustment

There are select at test resistors on each buffer amplifier, these are R17 and R32 for the two amplifiers and they are selected for best null.

4.2.6.2 Gain Balance Adjustment

The input resistors, R12, R15, R22 and R22 for the one amplifier and R28, R31, R36 and R40 for the second amplifier are selected to balance gains of all Hall generators. This is done by chosing a reference pole, and using this reference pole of the rotor, adjusting all amplifier gains such that the outputs due to the reference pole are equal.

4.2.6.3 After the gain balance adjustment is made, the spacing between the null positions of the sine and cosine channels will be checked. If it is not exactly 90^{o}, adjustment of the gain of one Hall generator will be made such that an exact effective 90^{o} spacing occurs.

4.3 Resolver-To-Digital Circuit Description

4.3.1 Resolver-To-Phase Converter

The carrier frequency has already been previously chosen to be 1200Hz. In the R-C networks, $R=X_{C}$ at 1200Hz. R is chosen at approximately 20K. Solving for C gives approximately 0.0068 ufd. For C exactly 0.006800, R comes out to 19.504K . The capacitors are Teflon dielectric types with a temperature coefficient of 70 PPM/^{o}C, and with much closer tracking between units. For the present requirement of $50^{o}C \pm 10^{o}C$, the capacitance variation will be ± 0.0007 or $\pm 0.07\%$. The tracking between two capacitors will be about 5 times better or, approximately $\pm 0.014\%$. The input signals are 5V peak at maximum coupling and the outputs are 3.5 VP variable phase signals.

4.3.2 Phase Meter

The phase meter consists of two zero crossing detectors (ZCS's). Parametersimportant for a zero crossing detector are constant high input impedance, low phase shift, and low offset. It is necessary to have a "bounding" circuit to keep the impedance high over portions of the cycle where the input is high, since the gain is very high. The bound circuit prevents amplifier saturation.

The ZCD shown is a tested design, with extremely high input impedance (10^{11} ohms). The following is a summary of characteristicsof the ZCD, over the temperature range -25^{o} to $+70^{o}$C.

A. Phase shift 0.0014 rad (0.082^{o})
B. Null = 0.003 mv. (Input Signal = 3.5V peak)

The ZCD is connected in the non-inverting configuration for high input resistance and has a gain of 100. The bound circuit consists of CR 3, 4, 5, 6, 7, 8, plus the associated resistors. The amplifier is a hybrid type containing JFET input stage. Following this is a μA710 compensator, used open loop, to sharpen the slope. The total gain is thus 100 x 1500 or 150,000. The μA710 output goes thru its complete range for $\frac{3.5}{150,000} = 23 \times 10^{-6}$ volts at its input.

4.3.3. Reset and Interrogate Pulse Requirements and Output Format

The two pulses from the ZCD's go to the binary counter circuit where they form the start and stop pulses for the counter. In operation, once on external enable pulse is received, a flip-flop will be set and upon receipt of start pulse, clock pulses begin to enter the counter. When the stop pulse occurs, the count will stop accumulating. Thus the phase (or the time) between start and stop pulses will be converted into a proportional count. The stop pulse also goes to a monostable consisting of a TTML9601 which generates a delay. This delayed pulse serves as a "Data valid pulse") indicating that the number in the counter is valid and ready for transmittal. A reset input is provided so that the counter can be reset after the number has been transferred and received.

4.4 Error Sensitivities

A study of error sensitivities of a resolver encoder such as the one described had been made in MT-14,008. The results in summary are:

4.4.1 RC Product Error

If the RC resolver to phase network values are $R_1 C_1 = R_2 C_2(1+\epsilon)$, the electrical out put phase error is ϵ radians.

In this recommended design, ϵ should be 0.00014, due to capacitor non-tracking. This will give a theoretical error of $\frac{0.00014}{6} = 0.00002$ radians or 0.00114 degrees mechanical.

4.4.2 ZCD Null

A null of V_n where the peak signal is V, gives rise to $\frac{V_n}{V}$ radians electrical.

In the present case where $V_n = 0.003$ and $V = 3.5$, the error is $\frac{0.003}{3.5} = 0.000856$ radians elect. This will give $\frac{0.000856}{6} = 0.000142$ radians or 0.0081 degrees mechanical.

4.4.3 ZCD Phase Shift

A ZCD phase shift is equal to the elctrical error directly. In the present case, the phase shift is 0.082 degrees electrical. The resulting error is $\frac{0.082}{6} = 0.014$ degrees mechanical.

4.4.4 Harmonic Distortion On Carrier

The effect of a harmonic distortion of d times the fundamental ($d < 1$), is to give an error of approximately d radians electrical. In the present case, the distortion will be about 0.00264 and the resulting error will be 0.00264 radians electrical or $\frac{0.00264}{6} = 0.00044$ radians (=0.025 degrees mechanical).

4.4.5 Total Electronic Error

The sum of the above errors is 0.048 degrees mechanical. The quantizing error is $\pm$ 1/2 bit or $\pm$0.58. By comparison the analog accuracy of the Hall resolver, after improvement by using multiple sensor, cannot be expected to be under 0.275 degrees.

Thus, the electronics have sufficient accuracy for the application.

4.4.6 Estimated Volume, Weight, and Power Consumption

The calculated values, based on the schematic are

volume	16 in^3
weight	4 oz.
power consumption	4 W total from +12 and -12V lines

5.0 CONCLUSIONS

Based on paper studies, the basic GFE error of 1.55 degrees can be improved. The limit of improvement appears to be 0.27 degrees. The electronics and Hall sensors are designed in a manner to perform this improvement. The expected error is approximately 0.5 degrees. This is less than 1 part in 2^9.

6.0 RECOMMENDATIONS

A suggested course of further action would begin with building and testing the proposed design to verify the multiple Hall sensor concept experimentally.

The second important area is the development of the magnetic structure. This involves evaluation of different magnetic structures to determine magnet materials, magnetic fixturing details, etc., to obtain the best sinusoidal spatial flux distribution. Involved here is a combination study and laboratory development. One of the main goals of such a program would be to see if the theoretical advantage of increasing the number of poles is actually available as an error reduction scheme.

7.0 REFERENCES

1. MT-14,008, "Analysis of Angular Errors Of A Type Of Digital Shaft Encoder", August 1, 1966, S. Malkiel.

2. MT-14,621, "Multiple Hall Generators For Hall Resolvers", October 23, 1969, S. Malkiel.

3. MT-14,620, "Sources Of Hall Resolver Errors", September 16, 1969, S. Malkiel.

4. MT-14,609, "Hall Resolver Test Report", H. Swanson November 10, 1969.

FILE COPY

To: Engineering File - MT-14,008
From: Saul Malkiel

Issue: Original
Date: August 1, 1966

Analysis of Angular Errors of a Type of Digital Shaft Encoder

Prepared by: Saul Malkiel
Saul Malkiel

THE BENDIX CORPORATION
ECLIPSE-PIONEER DIVISION
TETERBORO, NEW JERSEY

TABLE OF CONTENTS

1.0 INTRODUCTION

This report summarizes the results of a study aimed at determining the error sensitivity to certain parameter variations of a certain type of digital shaft encoder, exclusive of digital errors. The encoder in question uses a resolver whose electrical signals are fed to resistance-capacitance phase-shift networks which convert the variable-amplitude resolver outputs to two variable phase, constant amplitude signals. The phase difference between the two is then detected by two zero-crossing detectors. The start and stop signals generated by the zero-crossing of two variable phase signals are used to allow pulses from a clock to accumulate into a register. The count then is indicative of the shaft position, and ideally is linear with shaft position. The present report seeks to determine causes and extents of non-linearities. The system uses a dual speed resolver but the high speed portion determines the accuracy. Errors considered below do not include those due to resolver non-linearity itself.

Requirements upon the RC network, allowable excitation distortion, frequency stability and zero-crossing detector stability to meet a specified accuracy have been determined. Most of the error sensitivities have been determined on a "per count" basis, that is, they cause a one count error in the output and are, therefore, equal to the resolution limit.

2.0 DESCRIPTION OF OPERATION

The high speed portion of the digital shaft encoder system is shown in block diagram of Figure 1.

The timing section comprises an oscillator which typically would be a high quality quartz crystal type. The oscillator feeds a wave shaper which delivers a well-defined square wave to the frequency divider. The frequency divider output square wave will be filtered to sine wave in the wave shaper and then amplified to drive the resolver excitation windings. It is expected that inverse feedback will be required from the resolver to the amplifier input to keep distortion low.

The resolver secondaries are connected to the start and stop RC networks. Each of the two RC outputs is a constant amplitude signal, at the excitation frequency, with phase angle with respect to excitation proportional to mechanical rotation. One output leads with increasing input rotation while the other lags. In a 32 speed system each output changes 360 degrees electrical phase for $1/32 \times 360^{o} = 11.25^{o}$. The differential phase between the two, therefore, will reach 360^{o} at one half of 11.25^{o} or 5.625^{o} mechanical input rotation and there would be 64 ambiguities in a full 360^{o} rotation. The coarse resolver and associated circuitry will eliminate the ambiguity.

The two zero-crossing detectors together with their associated flip-flops produce a pulse train whose "on" time represents the phase difference, and gating with the clock

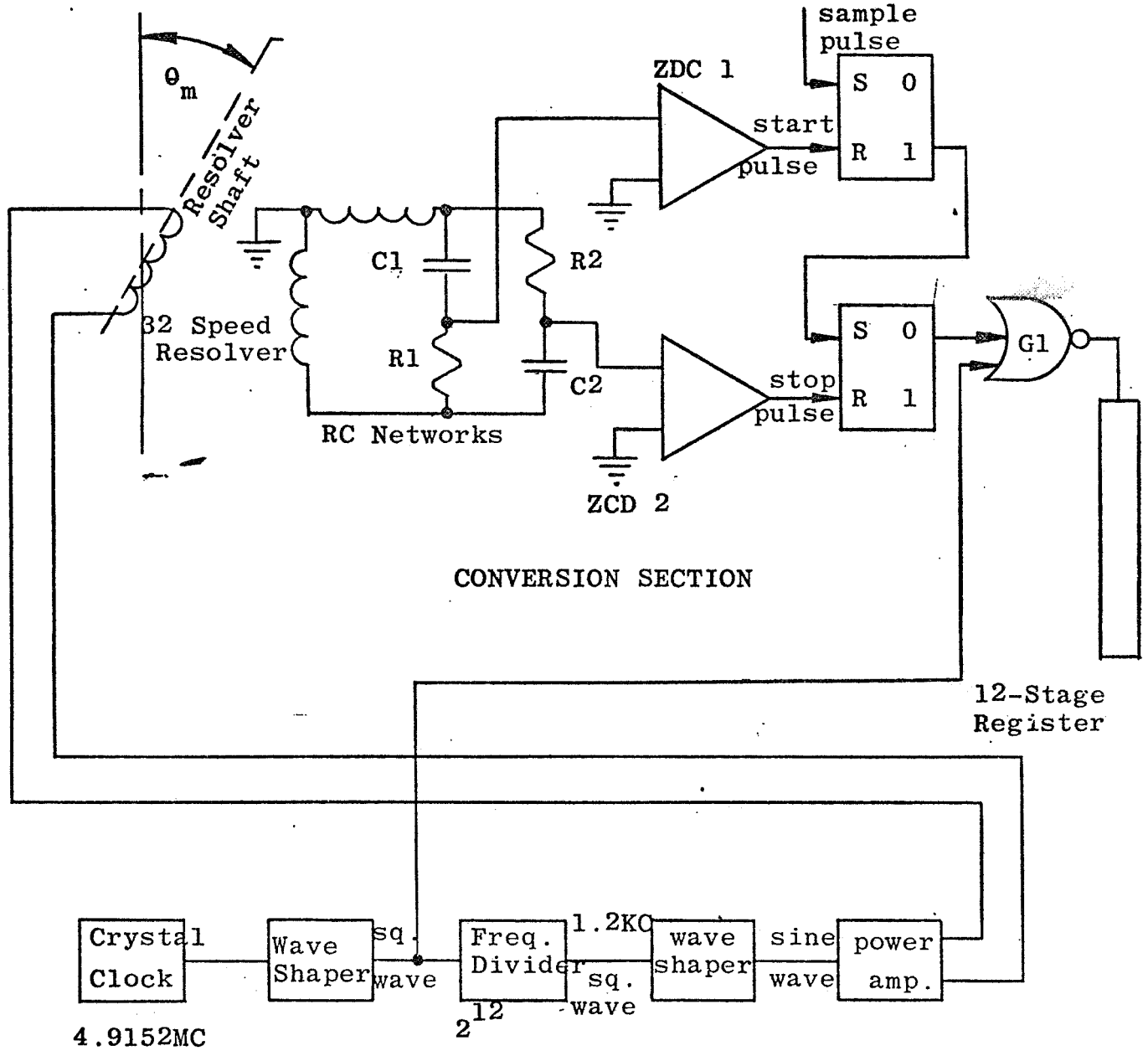

BLOCK DIAGRAM - DIGITAL SHAFT ENCODER

FIGURE 1

frequency allows clock pulses into the register. The binary number accumulated each scanning time represents mechanical rotation over a typical rotation segment of 5.625^{o}. Additional circuitry covering counter clearing and the low speed converter have not been shown.

3.0 ANALYSIS

3.1 ELECTRICAL OUTPUT VS. ROTATION

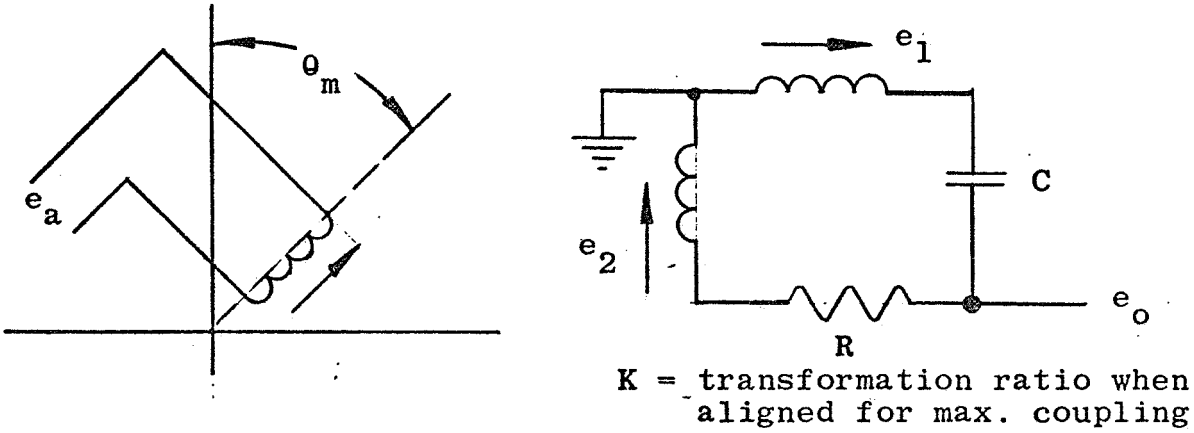

K = transformation ratio when aligned for max. coupling

FIGURE 2

Assume:

1. Zero source impedance to RC network
2. Ideal resolver
3. No load on RC network

$$e_o = e_1 \frac{R}{R + \frac{1}{j\omega C}} - e_2 \frac{\frac{1}{j\omega C}}{R + \frac{1}{j\omega C}} \qquad (1)$$

$$e_1 = e_a K \sin \theta_m \qquad (2)$$

$$e_2 = e_a K \cos \theta_m \tag{3}$$

$$e_o = e_a K \left(\frac{R \sin \theta_m - \frac{1}{j\omega C} \cos \theta_m}{R + \frac{1}{j\omega C}} \right) \tag{4}$$

$$e_o = \frac{e_a K}{j\omega CR + 1} \left(j\omega RC \sin \theta_m - \cos \theta_m \right) \tag{5}$$

Assume $\omega CR = 1$

$$e_o = \frac{e_a K}{j+1} \left(j \sin \theta_m - \cos \theta_m \right) \tag{6}$$

$$e_o = \frac{e_a K (\sin^2 \theta_m + \cos^2 \theta_m)^{1/2}}{(1^2 + 1^2)^{1/2}} \frac{\angle \tan^{-1} \frac{\sin \theta_m}{-\cos \theta_m}}{\angle +45^\circ} \tag{7}$$

Since for θ_m in the first quadrant, the angle of the numerator term is in the second quadrant, the phase angle may be written

$$\angle 180^\circ - \theta_m - 45 = \angle 135 - \theta_m$$

$$e_o = \frac{e_a K}{\sqrt{2}} \angle 135^\circ - \theta_m \tag{8}$$

Equation 8 states that the output of the resolver RC chain is a signal of constant amplitude, with phase advance linear with mechanical rotation. In the case of the present system, with dual RC networks and 32 speed resolver,

the phase difference will advance through its complete 360 degree range within a range of mechanical motion of $\frac{360}{64} = 5.625^{o}$. The number 135^{o} in Equation 8 is somewhat arbitrary and is due to the coordinate system reference chosen.

3.2 ERROR DUE TO WRC $\neq 1$

It is of importance to determine the accuracy required of the network components to meet a certain encoding accuracy:

Assuming $\omega RC = 1 + \epsilon$, and checking at $\theta_m = +135^{o}$,

$$e_o = \frac{e_a K}{j\omega CR+1} \quad (j\omega RC \sin \theta_m - \cos \theta_m). \tag{1}$$

Since at $+135^{o}$, and also at -45^{o}, $\sin \theta_m = -\cos \theta_m$, the above reduces to

$$e_o = \frac{e_a K}{j\omega RC+1} \left(j\omega RC \left[+.707\right] - \left[-.707\right]\right) = \tag{2}$$

$$e_o = e_a K \ (.707) \tag{3}$$

This expression is completely independent of RC product. The physical significance is that the rotor is aligned so as to couple equal voltage into the two stator windings. No current flows in the RC network and the RC network output is equal to the RC network input. In a similar manner at $\theta_m = -45^{o}$, the output is of -180^{o} phase but completely independent of RC values.

To evaluate the error, the following analysis is used.

$$d(\tan^{-1}x) \quad , \quad \frac{dx}{1+x^2} \tag{5}$$

where

$$\Delta\theta = d(\tan^{-1}x) = -\frac{1}{1+1^2} = -\frac{\epsilon}{2} \tag{6}$$

The total phase error must be the sum of the effect of both $\angle\tan^{-1}$ terms and is, therefore, $-\frac{\epsilon}{2}-(\frac{\epsilon}{2}) = -\epsilon$ radians.

Evaluation at $\theta_m = -135^o$

$$e_o = \frac{e_a K}{j(1+\epsilon)+1}\left(-j\left[.707\right]\left[1+\epsilon\right] - \left[-.707\right]\right) = \tag{7}$$

$$= \frac{.707\ e_a K}{j(1+\epsilon)+1}\left(+1 - j\left[1+\epsilon\right]\right)$$

$$e_o = \frac{.707\ e_a K\sqrt{1+(1+\epsilon)^2}}{\sqrt{1+(1+\epsilon)^2}} \quad \frac{\angle\tan^{-1}-(1+\epsilon)}{\angle\tan^{-1}(1+\epsilon)} \tag{8}$$

The vector diagram for this case is below in Figure 4 and shows that the error is also negative. The magnitude is also ϵ radians.

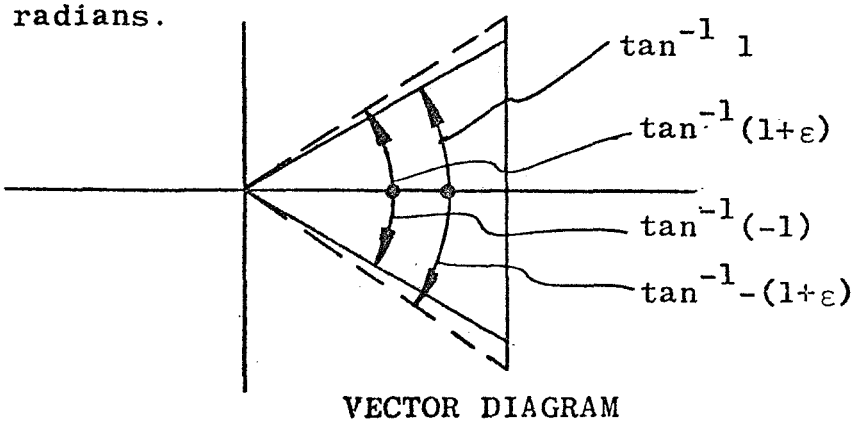

VECTOR DIAGRAM

FIGURE 4

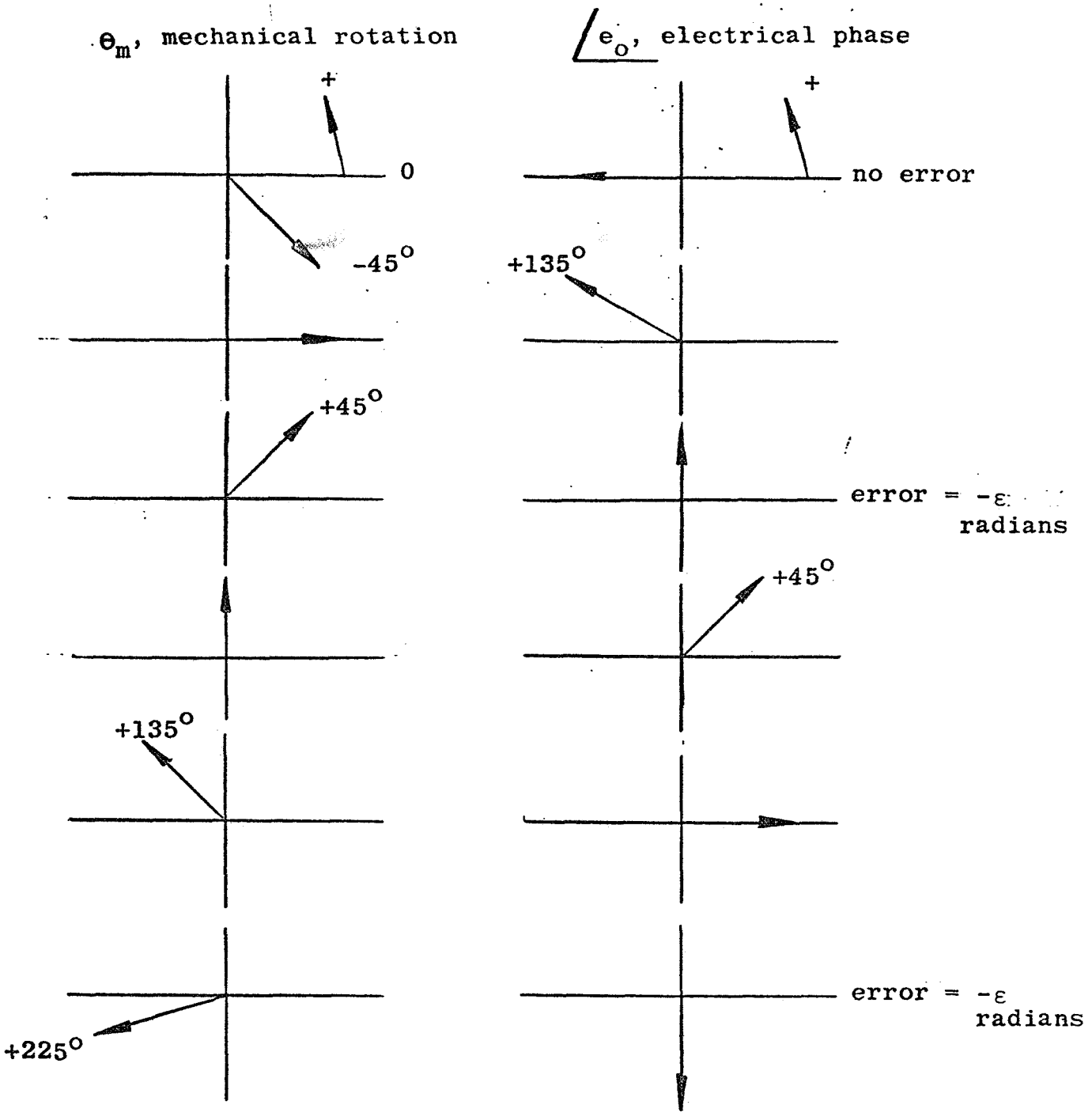

ELECTRICAL PHASE VERSUS MECHANICAL ROTATION, COARSE RESOLVER

FIGURE 5

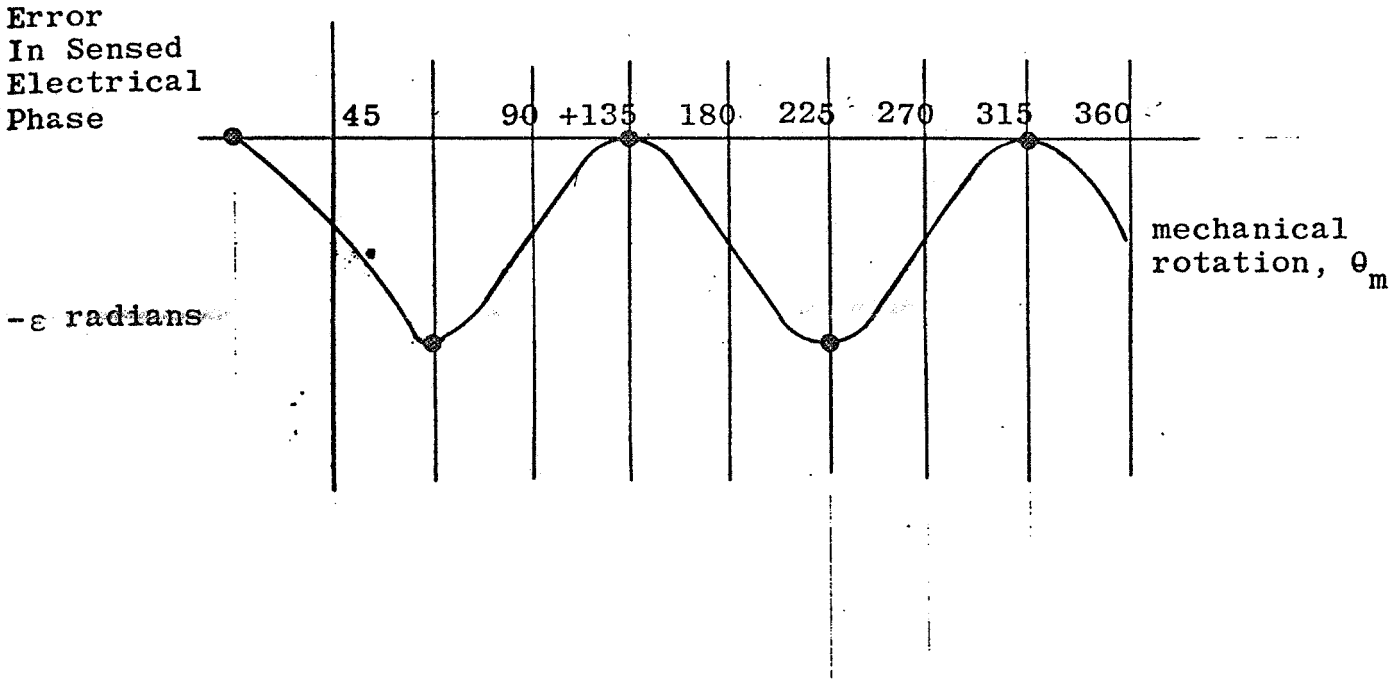

PLOT OF PHASE ERROR VS. ROTATION FOR RC = 1 + ϵ

FIGURE 6

Figure 6 is the graph of electrical phase error at various rotation angles, for a single speed resolver. Since in this case electrical phase and mechanical rotation angles are commensurate, it also represents mechanical errors.

Extension to High Speed Resolver with 2 R-C Networks

The plot of both R-C outputs versus rotation is shown in Figure 7. At $135^{\circ} = \theta_m$, both outputs are in-phase. This together with the fact of opposite slopes determines the plot of the second R-C output. Super-imposed is shown the effect of ϵ.

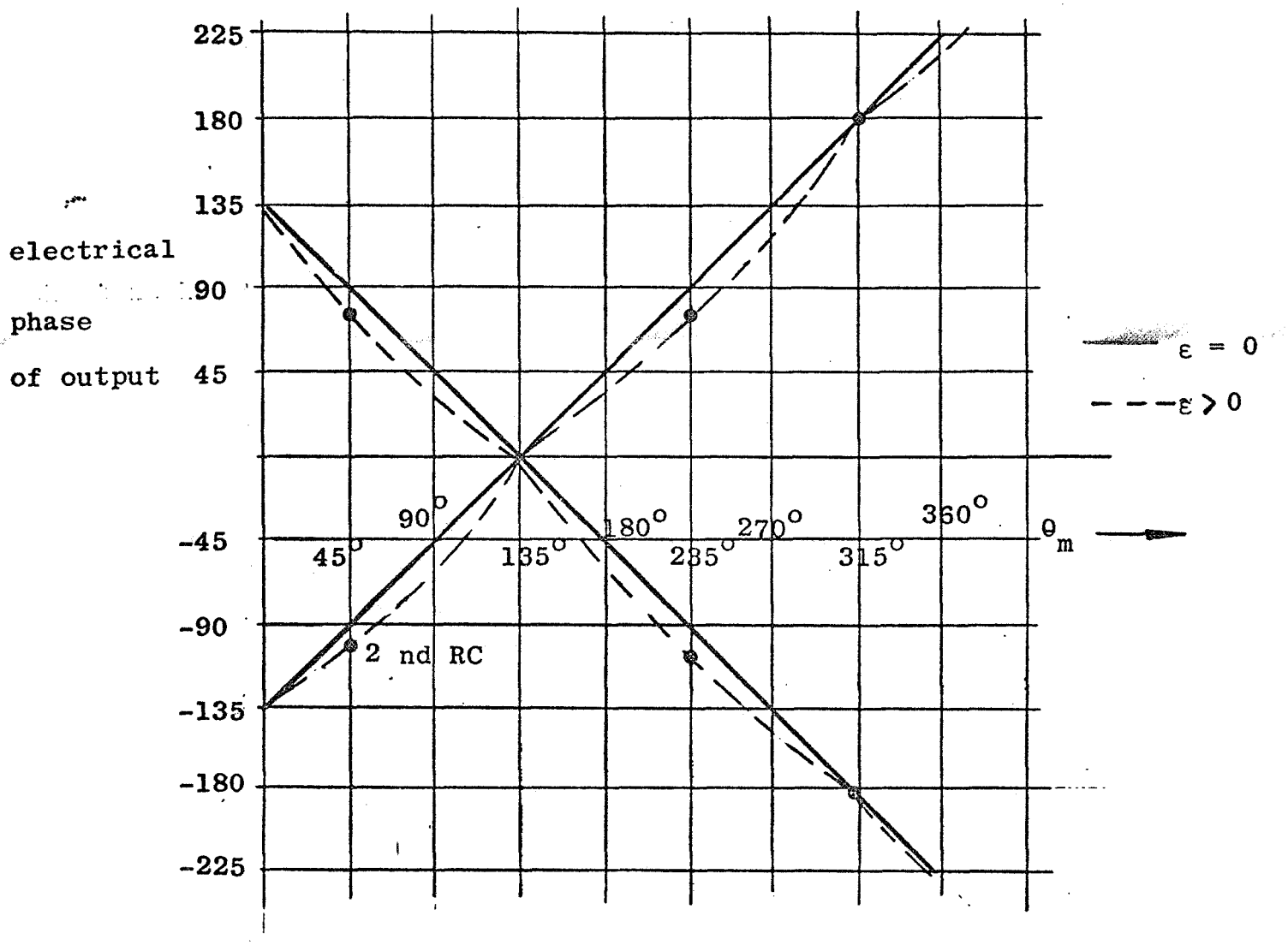

FIGURE 7

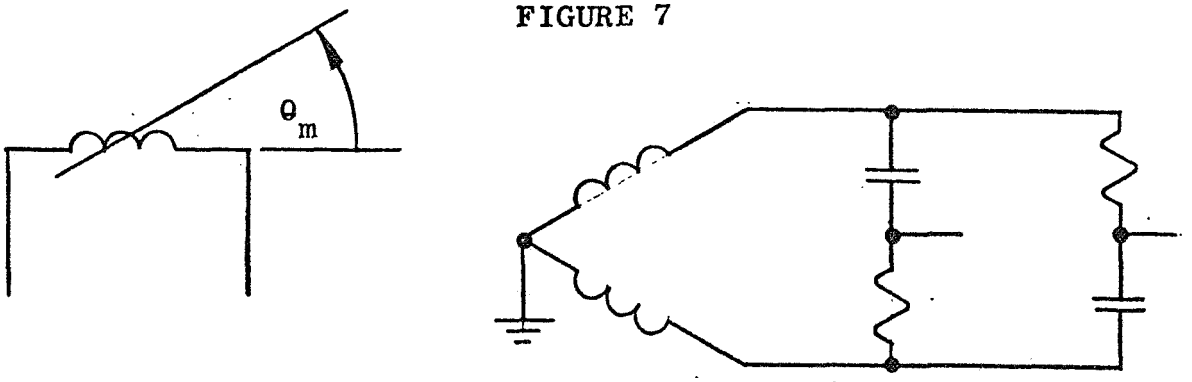

FIGURE 8

In Figure 8 it is seen, using a new reference system (135° displaced), that the output of RC 2 at angle $-\theta_m^1$ is equal to the output of RC1 at $+\theta_m^1$. In the Figure 7 plot of RC1 the fact that the curve for ϵ 0 lies below that for $\epsilon = 0$ is corroborated physically by the fact that there must be 180° difference between the output of one network with a given θ_m^1 and with $\theta_m^1 + 180$. Also, the fact that both plots show negative errors due to ϵ throughout is corroborated by the physical reasoning which says that, with $e^{>o}$, the output of RC1 at θ_m^1 must be the same as the output of RC2 at $-\theta_m^1$. This points up the conclusion that ϵ errors common to both RC sections are self-compensating and that only tracking of $\epsilon_1 = \omega R_1 C_1$ with $\epsilon_2 = \omega R_2 C_2$ is of importance. In the presence of $R_1C_1 = R_2C_2$ there is also no sensitivity to frequency change.

The error due to one RC network being perfect and the other containing error must be considered. For a coarse system the phase and mechanical errors are both equal to ϵ radians. In the present system, the required resolution is one part in 2^{18}. This will be composed of one part in 2^6(64) due to selecting one of the 64 high-speed sections, together with one part in 2^{12}(4096) resolution of each section. The resolution steps are, therefore, $\frac{360}{2^{18}} = .0014$ mechanical degrees overall. Each RC network output phase has a $\frac{\text{phase degrees}}{\text{mech. rotat.}} = 32$, and, therefore, has a phase output of .0014 x 32 = .045 degrees, or .0008 radians. The phase difference will be double this and will be .0016 radians, a value, whose time delay is .2 x 10^{-6} sec., the pulse spacing. Working backward, it would require the full .0016

radians error at one phase due to $\epsilon \neq 0$, to develop a one bit error. The requirement on one RC phase, for one bit error is, therefore, that $\epsilon = .0016$ or less. This may be generalized in view of the preceeding argument that the differences in ϵ_i, ϵ_1 and ϵ_2, the values for the two network phases, shall be less than 0.0016. On a practical basis, the requirement is that the second RC network must be specified to track the first to this deviation.

3.3 ERROR DUE TO ZERO CROSSING DETECTOR IMPERFECTIONS

3.3.1 Detector Input Impedance

3.3.1.1 Analysis of Network

Assume the detector has an input resistance equal to R_L.

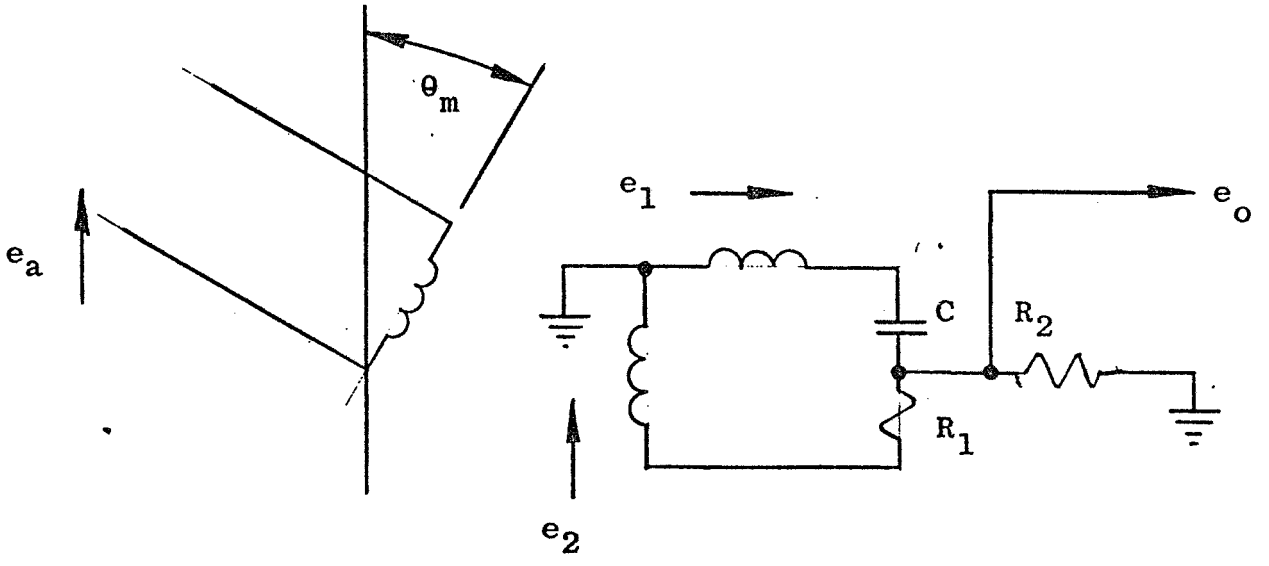

FIGURE 9

$$e_o = e_1 \frac{\frac{R_1 R_L}{R_1 + R_L}}{\frac{R_1 R_L}{R_1 + R_L} + \frac{1}{j\omega C}} - e_2 \frac{\frac{R_L \frac{1}{j\omega C}}{R_L + \frac{1}{j\omega C}}}{R_1 + \frac{R_L}{j\omega C}} \qquad (1)$$

$$\begin{cases} e_1 = e_a K \sin \theta_m \\ e_2 = e_a K \cos \theta_m \end{cases}$$

$$e_o = e_1 \frac{R_1 R_L}{R_1 R_L + \frac{R_1 + R_L}{j\omega C}} - e_2 \frac{\frac{R_L}{j\omega C}}{R_1 (R_L + \frac{1}{j\omega C}) + \frac{R_L}{j\omega C}}$$

(2)

$$e_o = e_1 \frac{j\omega C R_1 R_L}{j R_1 R_L \omega C + R_1 + R_L} - e_2 \frac{R_L}{R_1 R_L j\omega C + R_1 + R_L}$$

(3)

$$e_o = e_1 \frac{j\omega C R_1}{j\omega C R_1 + \frac{R_1}{R_L} + 1} - e_2 \frac{1}{j R_1 \omega C + \frac{R_1}{R_L} + 1} \qquad (4)$$

$$e_o = \frac{(e_1 j\omega C R_1 - e_2)}{j\omega C R_1 + 1 + \frac{R_1}{R_L}} \qquad (5)$$

Assume $\omega R_1 C = 1$

$$e_o = \frac{je_1 - e_2}{j + 1 + \frac{R_1}{R_L}} = \frac{e_a K \left[j \sin \theta_m - \cos \theta_m \right]}{j + 1 + \frac{R_1}{R_L}} \qquad (6)$$

$$\text{Amplitude of } e_o = \frac{e_a K \sqrt{\sin^2 \theta_m + \cos^2 \theta_m}}{\sqrt{1 + \left(1 + \frac{R_1}{R_L}\right)^2}} = \frac{e_a K}{\sqrt{1 + \left(1 + \frac{R_1}{R_L}\right)^2}} \qquad (7)$$

$$\text{phase of } e_o = \tan^{-1}\left(- \frac{\sin \theta_m}{\cos \theta_m}\right) - \tan^{-1} \frac{1}{1 + \frac{R_1}{R_L}} \qquad (8)$$

The phase error, due to loading, is a function of the second term and is the deviation of this term from $(-\frac{\pi}{4})$ rad. It is obviously independent of rotation angle and is, therefore, a constant bias type of error. Also, it may be balanced out by an equal error due to the second RC network. Thus it is only mismatch which causes error and a calculation of mismatch of loading with respect to the two zero crossing detectors is made below.

Phase error due to loading of one RC section = $\Delta\theta$ =

$$\tan^{-1} 1 - \tan^{-1} \frac{1}{1 + \frac{R_1}{R_L}}$$

$$\Delta_\theta \cong \tan \Delta\theta = \frac{1 - \dfrac{1}{1 + \dfrac{R_1}{R_L}}}{1 + \dfrac{1}{1 + \dfrac{R_1}{R_L}}} = \frac{\dfrac{R_1}{R_L}}{2 + \dfrac{R_1}{R_L}} \qquad (9)$$

$$\Delta\theta \cong \frac{1}{2\dfrac{R_L}{R_1} + 1} \qquad (10)$$

if $\frac{R_L}{R_1} = n$ and > 1, Equation 10 may be approximated by

$$\Delta\theta = \frac{1}{2n} \quad \text{or} \quad n = \frac{1}{2\Delta\theta} \qquad (11)$$

The error in phase radians, for each phase, for one bit error, has been shown to be .0016 radians.

Differentiating Equation 11 above,

$$d\Delta\theta = \frac{1}{2}\frac{dn}{(-n^2)} = -\frac{1}{2n}\frac{dn}{n} \qquad (12)$$

since $d\Delta\theta = .0016$, and also $\frac{dR_L}{R_L} = \frac{dn}{n}$

$$.0016 = -\frac{1}{2n}\frac{dR_L}{R_L} \quad \text{or} \quad \frac{dR_L}{R_L} = -.0032\ n \qquad (13)$$

Figure 11 shows the graph of Equation 13. It is seen that larger values of n, the loading parameter, tolerate larger inaccuracies in R_L. This graph may be used when designing a ZCD, to determine the amount of feedback required, and may be read as a mismatch requirement on the two ZCDs.

It is of interest to note what the error is at n = 5 which represents R_L = 100,000 and $R_1 = X_C$ = 20,000, a previously proposed arrangement. The $\frac{dR_L}{R_L}$ for one bit is, from the curve, 0.016. The instrumentation required would be Figure 10B with input resistor equal to 100,000 ohms and feedback resistance low enough to provide the above input impedance stabilization.

In Figure 10A is shown a connection of a differential amplifier to give a high input impedance. This device behaves much like an impedance multiplier raising the intrinsic impedance by a constant factor. It, therefore, does not change the ratio $\frac{\Delta R_L}{R_L}$ where ΔR_L is the variation in input resistance with temperature. Figure 11 shows however, that this device is suitable as a ZCD in this application because at high R_L, $\frac{\Delta R_L}{R_L}$ may be large.

Both configurations, therefore, appear to be suitable and a more rigorous analysis might be expected to show an actual electrical equivalence. "Bound" circuits are shown which are necessary to prevent saturation of the amplifier which would require an overload recovery time, showing up as a phase shift.

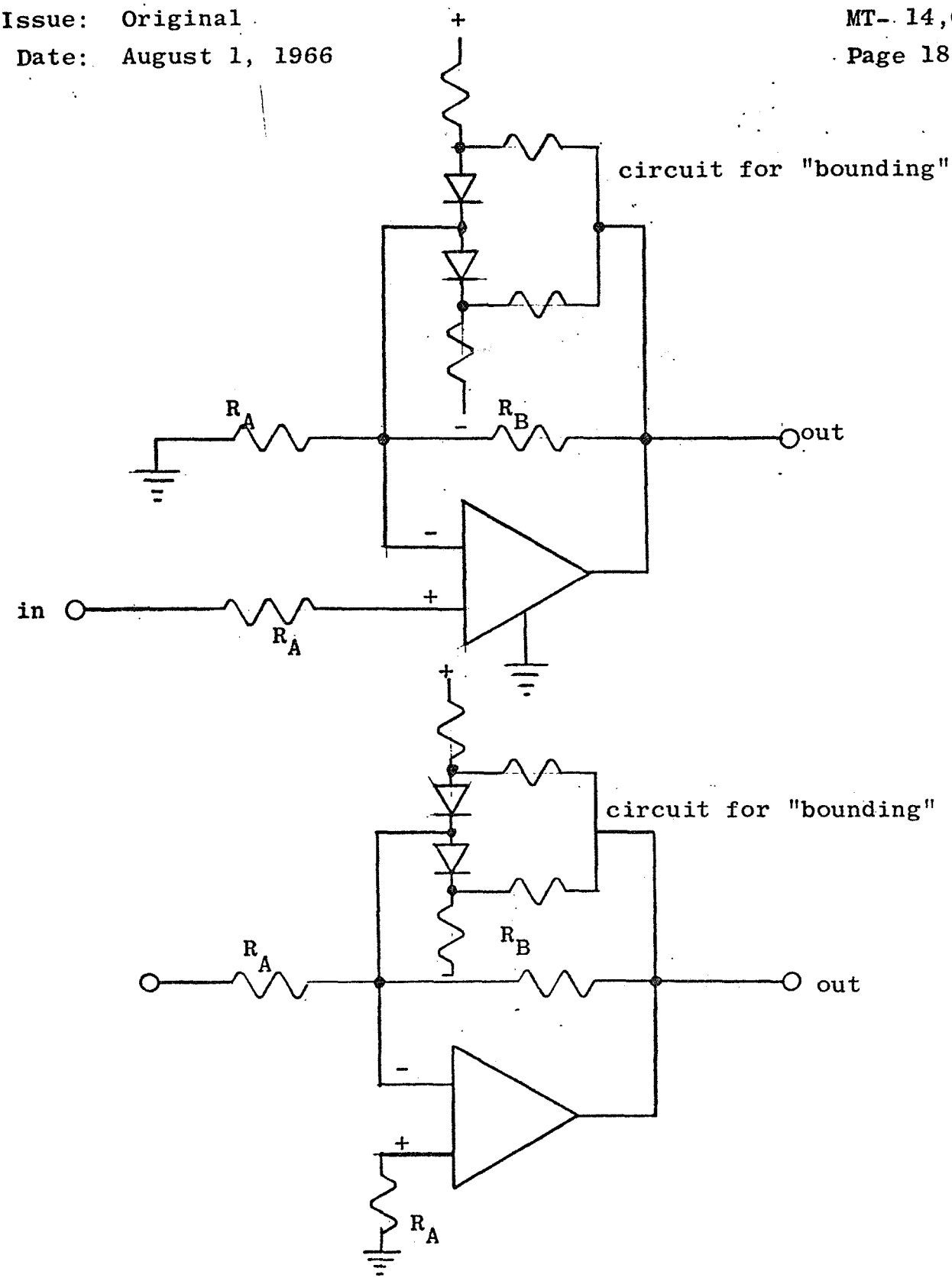
+
circuit for "bounding"
R_A
R_B
-
out
-
in
+
R_A
+
circuit for "bounding"
R_B
R_A
out
-
+
R_A

FIGURE 10

ERROR SENSITIVITY
ZCD Input Resistance
FIGURE 11
fractional change in R_L
$\frac{dn_T}{n_T} \div \frac{dR_L}{R_L}$
n = loading parameter
.108
.096
.084
.072
.060
.048
.036
.024
.012
8
16
24
32
40
48
64
80
96

3.3.2 Error Due to Drift of ZCD

The ZCDs are direct coupled devices and possess drift rates which are due to random and temperature-induced effects.

If 5 VRMS = resolver output at maximum coupling, then $\frac{5}{\sqrt{2}} = 3.53$ volt = network output. For a one bit error or 0.0016 radians phase error per phase, the .0016 x 3.53 x 1.4 = .0080.

A drift stability of ± 8 millivolt which would represent an encoding drift just equal to the resolution available appears to be just possible using microelectronic differential amplifiers. Again this statement may be generalized to represent the tracking required between the two ZCDs.

3.3.3 ZCD Phase Accuracy

The ZCDs receive 1200 CPS inputs and are required to faithfully reproduce the phase of these inputs. A phase lag at this frequency may also be expected to also make itself known by a changing lag with time or environment. The allowable phase tracking of .0016 radians is equal to $.09^{o}$. It is obvious that high frequency response devices must be used together with inverse feedback, to meet this phase stability.

3.3.4 Other Amplifier Considerations

The amplifier used as a ZCD will degrade the performance of the system to some extent. The shift of input impedance, phase shift, and zero, contribute as shown above. However,

distinct from these is a change in ZCD gain or output signal with some input signal. This will be caused by changes in feedback resistors and open-loop gain. But since the output of the ZCD is used only to indicate zero, or something very close to it, changes in slope are of very little concern. The component following the ZCD, which must also indicate zero, and which may be an amplifier or Schmitt trigger, has pulse-steepening as its main duty and changes in slope of the ACD produce only second order effects.

3.4 EFFECT OF HARMONICS OF RESOLVER EXCITATION

This section analyses the extent which distortion contributes to error.

For a signal $V = \sin 2\pi ft.$ (1)

The rate of change $= \frac{dv}{dt} = 2\pi f \cos 2\pi ft.$ (2)

At $t = 0$, $\frac{dv}{dt} = 2\pi f$ = slope at zero-crossing. (3)

Assume a harmonic voltage or noise voltage of e volts is present at zero-crossing. This will shift the time of zero-crossing by an amount depending upon e and the slope $2\pi f$. See Figure 12.

$\frac{e}{\Delta t} = 2\pi f$ from Figure 10 (4)

$f = \frac{1}{T}$ (5)

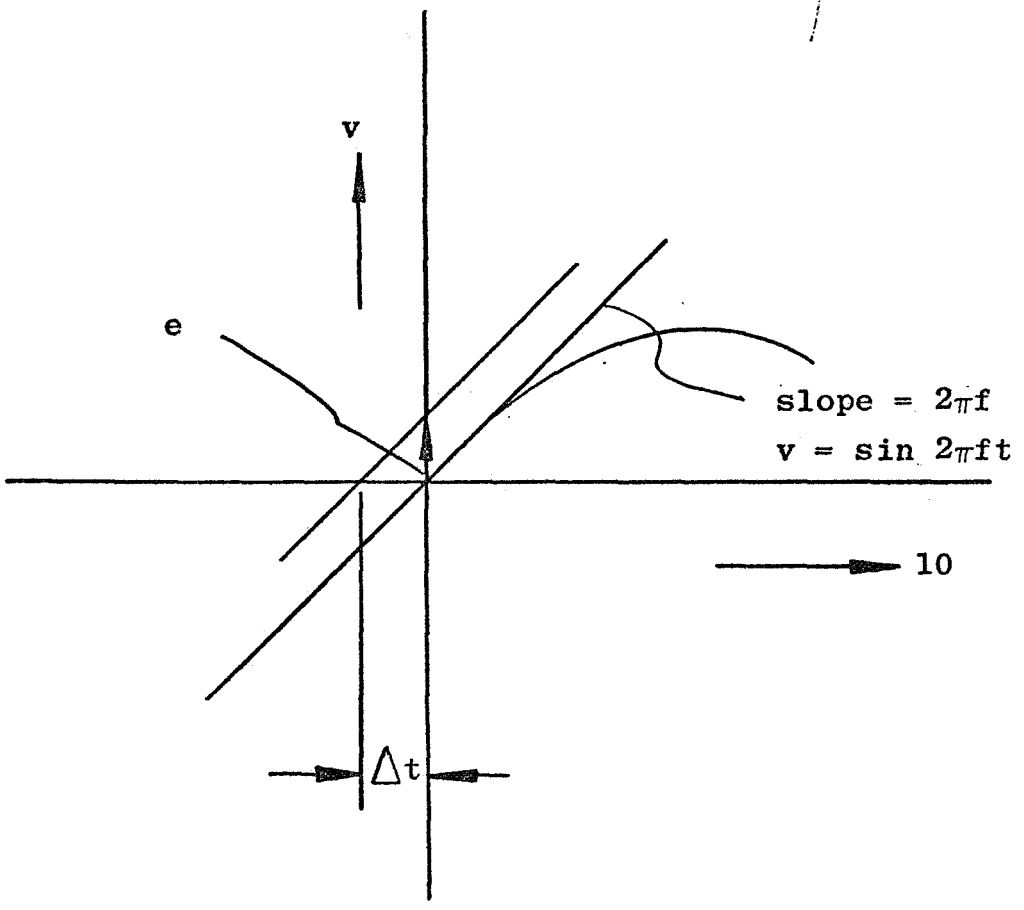

DETAIL OF WAVEFORM AT ZERO-CROSSING
FIGURE 12

$$\frac{\Delta t}{T} = \frac{e}{2\pi} = \frac{\Delta \phi}{2\pi} \tag{6}$$

but $\frac{\Delta t}{T} = \frac{\Delta \phi}{2\pi}$

$$\therefore \quad e = \Delta \phi \tag{7}$$

Equation 7 is for a single speed system and states that the fractional harmonic content equals the phase error out of a ZCD. This relationship is similar to that of Section 3.2. For one bit error, $\Delta \phi$ = .0016, which equals e, the relative distortion.

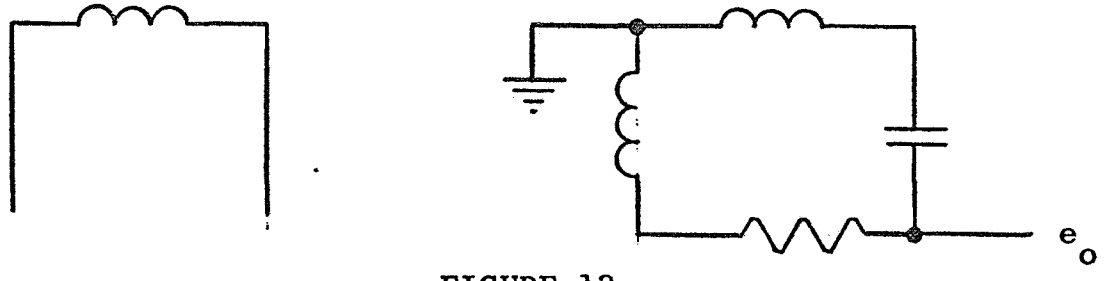

FIGURE 13

In the mechanical orientation of Figure 13, the coupling of third harmonic to the output is apparently greatest since full coupling is present in the leg which capacitively couples to the output. The third harmonic in the excitation will be assumed to be third harmonic of a phase as shown in Figure 14.

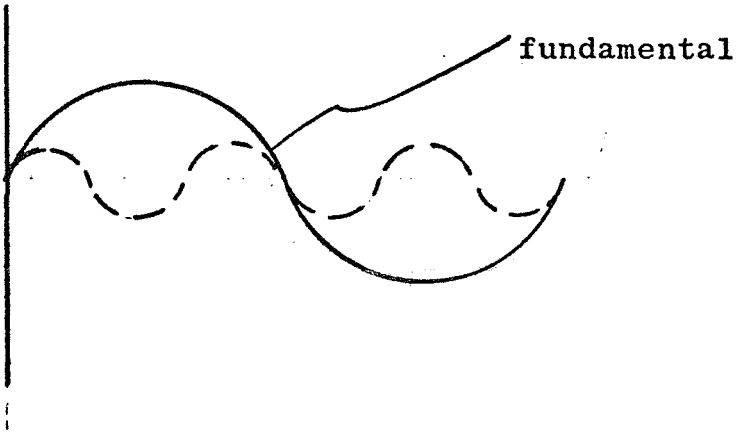

FIGURE 14

This is representative of imperfect forming of a sine wave from a square wave by filtering.

In the above orientation, the fundamental output is $+45^{o}$ of 0.707V output as previously computed, assuming one volt excitation. The third harmonic output is approximately unity output with a phase of $+\text{ctn}^{-1}$ 3 CR or $+18^{o}$ approximately. In terms of fundamental degrees of phase, this is $\frac{18}{3} = 6^{o}$. Thus the third lags the fundamental by 45-6 = 39 fundamental degrees. In terms of third harmonic phase degrees, this is 39 x 3 = 117^{o}. Since the sine of 117^{o} is approximately .866, the previous analysis must be modified by the factor $\frac{.866}{.707}$ to account for the effective relative amplification of the harmonic with respect to fundamental, and the previously determined number of .000764 must be modified to 0.0016 x $\frac{.707}{.866}$ = 0.0013; the error is a time lag in zero-crossing.

For the second RC network, under the same rotor orientation, the fundamental output is -45^{o}. The third harmonic trans-

mission under these conditions, is approximately $\frac{1}{3}$, and the phase is -72^{o}. See Figure 14.

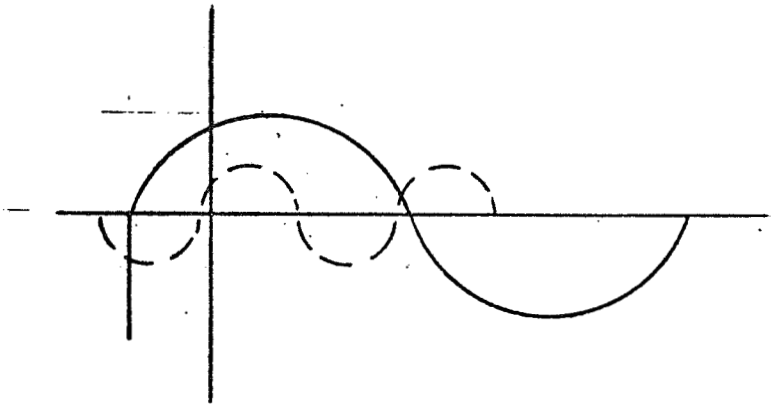

RC 1

FIGURE 15

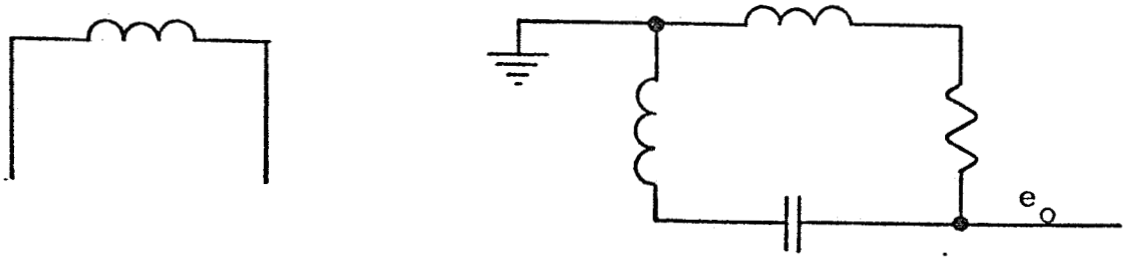

RC 2

FIGURE 16

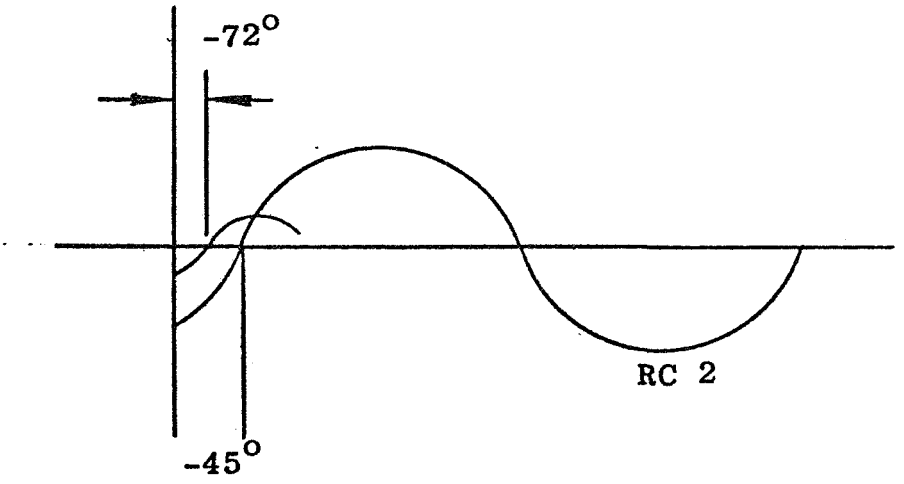

FIGURE 17

In terms of fundamental degrees, the -72° represents -24° fundamental phase lag. The third harmonic, therefore, leads the fundamental by 45-24 = 21 fundamental degrees. This is equivalent to 21 x 3 = 63 third harmonic degrees. The sine of 63° being approximately .866, it is seen that this network will have the time of zero crossing made early by the addition of the postulated third harmonic, and of a magnitude equal to that of the previously considered RC1 network. The allowable distortion, for one bit error is thus $\frac{.0013}{2}$ = .000651.

The above original assumption as to the phase of the third harmonic distortion due to imperfect filtering is somewhat arbitrary and the phase may not be as assumed. In order to account for the effect of a more adverse phase, the above results should be modified to allow the occurence of a third harmonic peak occurring at zero-crossing. Thus, a modifier of .866 should be used to give .00065 x .866 = .00056. This fractional distortion will meet the one bit error due to harmonics.

4.0 SUMMARY

The following summarizes the previous analysis.

1. The output of the resolver RC chain is a signal of constant amplitude, with phase advance linear with mechanical rotation. The high-speed double RC output difference signal repeats 0 to 360^{o} phase, 64 times for a 32-speed resolver.

2. Error due to RC variation from unity:

   On the coarse output, there are two points around the circle with no phase error due to RC deviation from unity. There are two other points where the maximum error occurs. These are between the two null error points and the phase errors are $-\epsilon$ radians, where $\omega RC = 1 + \epsilon$. Since in the coarse system phase errors in degrees are numerically equal to mechanical errors in degrees, the mechanical error maxima are $-\epsilon$ radians rotation maximum. In the high speed (32:1) resolver chain, a difference in the two ϵ for both networks of .0016 will result in a one bit error. For small shifts, there is no error due to frequency shift alone.

3. Errors due to ZCD input impedance:

   The error caused by finite ZCD input impedance is that of a constant phase error. If both ZCDs are matched in input impedances, then the constant phase error disappears due to the method of phase differencing used.

Figure 11 shows the matching accuracy required. For a rotation of load to network impedance equal to 5, both ZCD input resistances must be matched to each other to within 1.6%.

Since the graph shows that a larger change in resistance is permissable if high input impedances can be synthesized, a sample from the graph is noted. If n = 300, that is, input resistance equal to 6MΩ, a variation of ±90% in resistance may be tolerated before a one bit error results.

4. Error due to ZCD drift:

The error due to ZCD drift is ±8 millivolt difference between the two ZCDs. This appears to be obtainable using presently available microelectronic amplifiers over the required temperature range of -25° to $+85^{\circ}$C.

5. Phase requirement of ZCDs:

The required phase tracking between the two ZCDs is 0.09°. Inverse feedback probably will be needed around the ZCD amplifier to achieve this.

6. Error due to harmonic distortion of excitation:

The resolver excitation must contain a harmonic distortion of less than 0.056% for a one bit error. Distortion generated in the resolver itself will also cause error at the rate of one bit for 0.056%.

ZCD IMPERFECTIONS

	Error due to RC ≠ 1 (3.2)	Error due to input impedance mismatch of 2 ZCDs (3.3.1)	Error due to drift of ZCD (3.3.2)	Error due to phase change of ZCD (3.3.3)	Error due to harmonic distortion (3.4)
32:1 speed resolver	$\epsilon = .0016$ ($RC = 1+\epsilon$)	See Fig. 11 Examples: 1) with $\frac{R_L}{R_1} = 5$ $\frac{dR_1}{R_L} = 0.016$ 2) with $\frac{R_L}{R_1} = 300$ $\frac{dR_L}{R_L} = .9$	$\pm 8 \times 10^{-3}$V	0.09^{o} phase	0.056% distortion
higher speed resolvers	All errors will decrease in proportion to increase of numerical high speed ratio				
quantization errors	Quanta should only be small enough so as not to be limiting factor.				

GENERALIZED RESOLVER-TO-DIGITAL SYSTEM FACTORS

CAUSING ONE BIT $\frac{1}{2^{18}}$ ERROR

To: Engineering File MT 14,621 Issue: A

From: S. Malkiel Date: 19 November 1969

MULTIPLE HALL GENERATORS

FOR HALL RESOLVERS

Prepared by: S. Malkiel

S. Malkiel

THE BENDIX CORPORATION
NAVIGATION AND CONTROL DIVISION
TETERBORO, NEW JERSEY

Code: 09 22 02

REVISIONS

PAGE	A	B	C	D	E	F	G	H	I	J	K
COVER	X										
1											
2											
3											
4											
5	X										
6	X										
7											

1.0 INTRODUCTION

Non-sinusoidal space magnetization of rotors of Hall resolvers can be the major source of resolver error. This MT discusses an instrumentation using two Hall Generators per channel to reduce these errors.

2.0 GENERAL

A Hall resolver has a rotating permanent magnet inside a return path upon whose inner diameter is located two Hall generators. The Hall generators are oriented such that their sensitive axis is radial along the flux lines. They are spaced 90^{o} to each other (for a two-pole rotor). They are provided with a control current, making the output of one of the Hall generators proportional to sin (rotation) = sin θ, and the second proportional to cos θ, provided that the flux intensity versus θ is sinusoidal.

Various manufacturing limitations, especially in the magnet charging fixturing details, tend to give a rotor magnetization which is non-ideal. A usual case is one in which a third harmonic flux is the main distortion product. Assuming that the resultant distorted wave is symmetric about $\theta = \frac{\pi}{2}$, the phase of the 3rd harmonic is as shown in Figure (1). It may be seen that a peaked waveform is produced. This waveshape has been observed on tests of rotors in our laboratories. Changing the phase of the 3rd harmonic by 180^{o} will give a wave which is flattened on its top, rather than peaked, and which may also occur in practice.

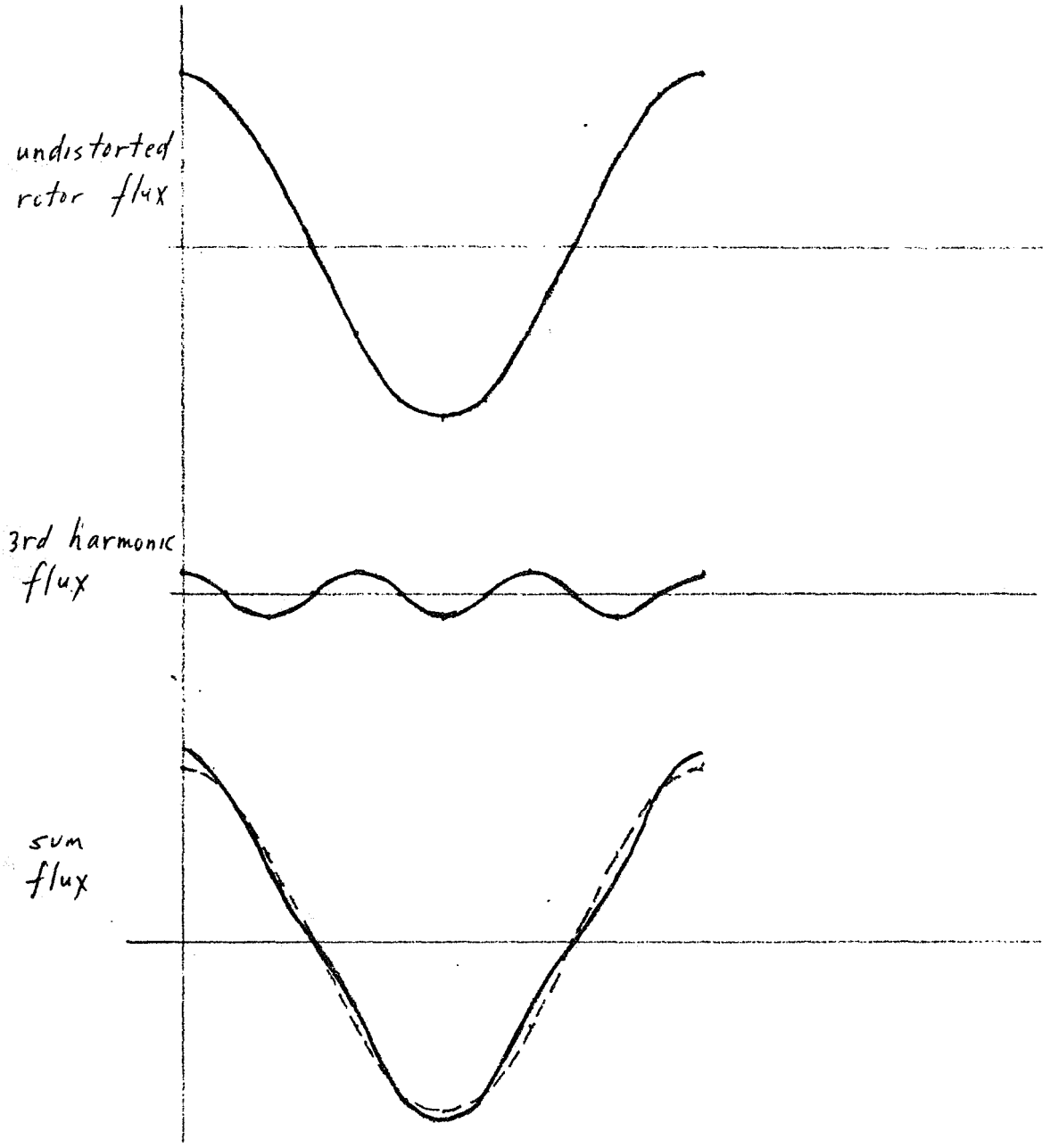

FIG. 1

WAVEFORM OF ROTOR FLUX WITH THIRD HARMONIC

Even though higher order harmonics may be also present, the 3rd will usually be the predominant error source, and elimination of it would give a large reduction in analog error of the resolver, so cancellation of higher harmonics will only be considered briefly.

3.0 CANCELLATION MEANS

Figure 2 shows a 2-pole resolver with the normal 0^{o} Hall generator replaced by two generators located 30^{o} to either side of 0^{o}. The 90^{o} generator has been divided similarly. Generators (1) and (2) have their outputs summed to give the sine output, using a summing amplifier, and generators (3) and (4) are similarly summed to obtain the cosine output.

Figure 3 explains, using vector diagrams, the 3rd harmonic cancellation. The horizontal component of the vectors at the left represents the output of generator (1) which is located at $+30^{o}$. To the right is the output of the -30^{o} sensor, (2) at the same time. It is seen that for any rotor position, the third harmonic vectors are equal and opposite. Therefore, summing of the two generators cancels out the third harmonic. The fundamental summed amplitude is 1.732 times the fundamental from either generator, as is the fifth harmonic.

4.0 TYPICAL CIRCUIT

Figure 4 shows a circuit which might be used with the two Hall generators per channel. The four Hall generators are connected in series to eliminate the effect of magneto resistance and of temperature coefficient of resistance.

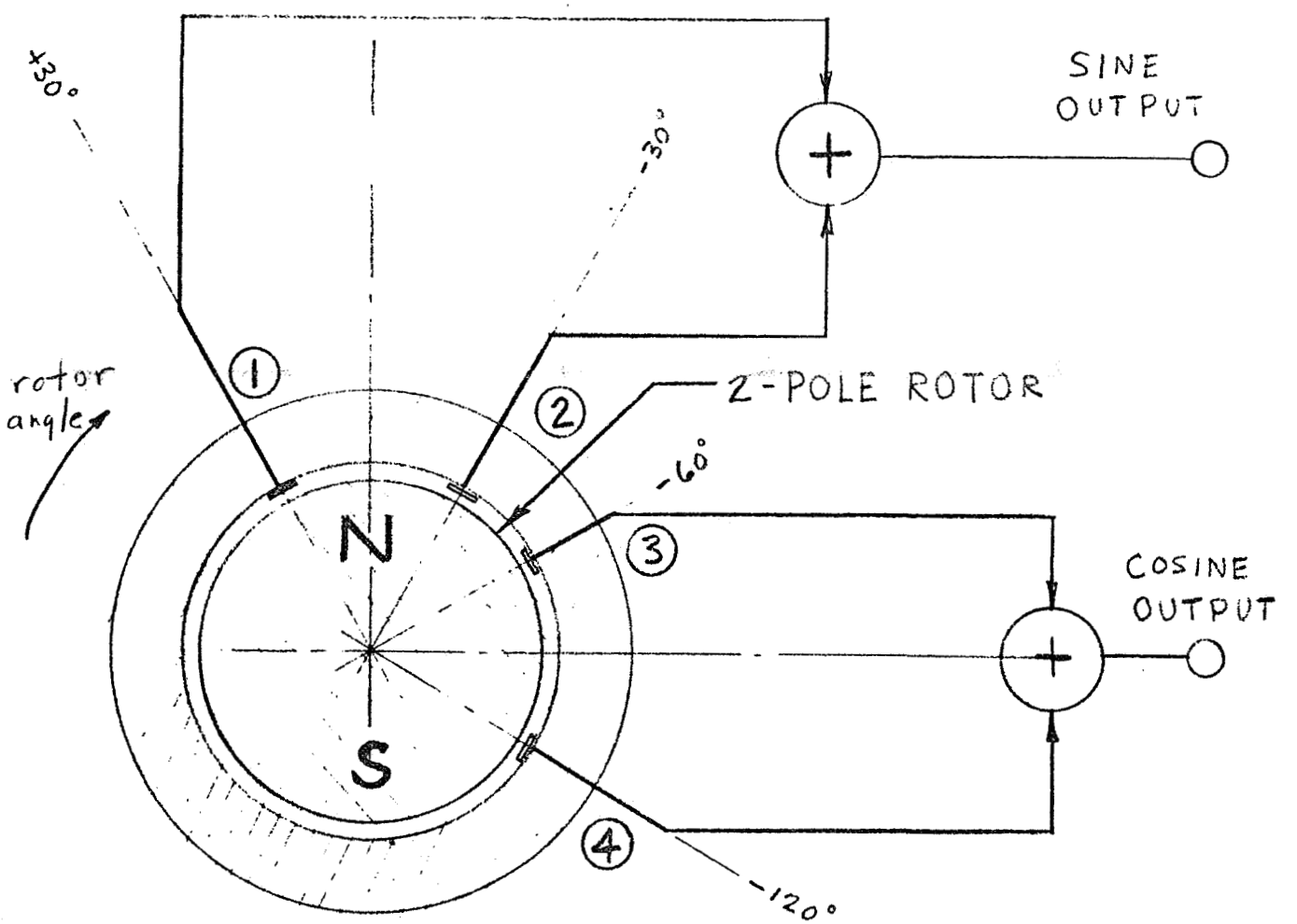

① ② ③ ④ HALL GENERATORS IN AIRGAP

FIG. 2

LOCATION OF MULTIPLE HALL SENSORS

FIG. 3 — CANCELLATION OF 3RD HARMONIC
SHOWING RESULTANT FUND. & 5TH HARMONIC

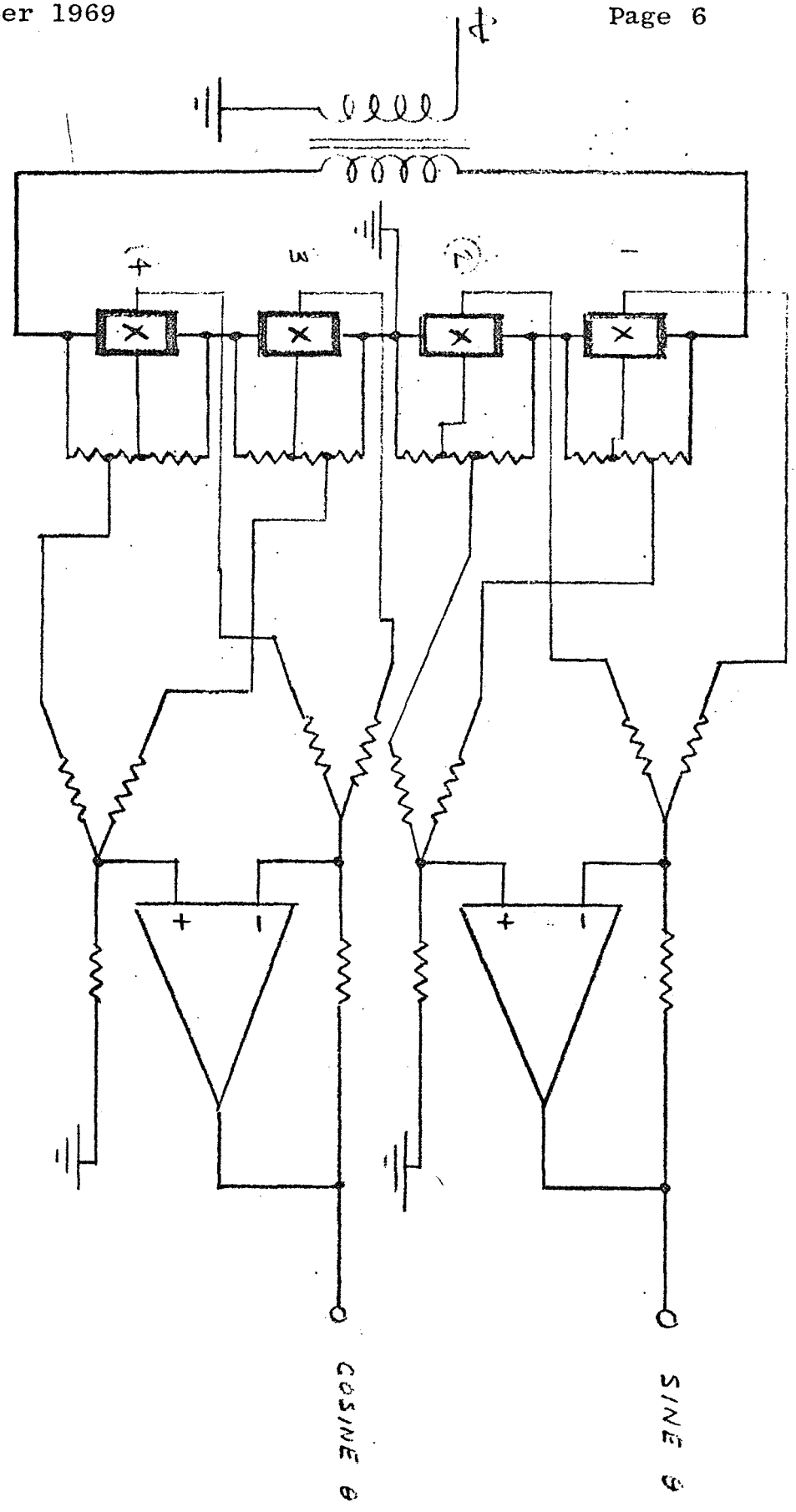

FIG. 4 - 3RD HARMONIC FLUX CANCELLATION CIRCUIT

A summing amplifier is used to combine the outputs of generators (1) and (2). Provisions will be made for adjustment of resistive nulls and for adjustment to take care of Hall generators of differing gains.

5.0 CONCLUSIONS

The foregoing offers a means to improve accuracy of a Hall resolver. The multiple sensor spacing of 60^{o} cancels the 3rd harmonic, leaving the 5th harmonic, if any, and the fundamental unchanged in relative magnitude to each other but multiplied by the factor $\sqrt{3} = 1.732$.

6.0 RECOMMENDATIONS

However, the added complexity is a disadvantage and in the production of high quality Hall resolvers it should be considered whether the above method should be preferred over methods in which effort is put into reducing the distortion at its source, i.e., at the magnet.

To: Engineering File - MT-14,620 Issue: Original

om: S. Malkiel Date: 16 September 1969

SOURCES OF HALL RESOLVER ERRORS

Prepared by: S. Malkiel
S. Malkiel

THE BENDIX CORPORATION
NAVIGATION AND CONTROL DIVISION
TETERBORO, NEW JERSEY

Code: 09 22 07

1.0 INTRODUCTION

In a Hall resolver, a rotating permanent magnet sweeps past two stationary Hall-effect generators. The Hall generators are flux-sensitive devices which give an output voltage proportional to the product of control current and flux. The control current may be DC or AC. Since the flux pattern on the magnet is sinusoidal with space, and assuming an AC excitation, for example , 1000 Hz, one Hall generator output is a 1000 Hz carrier, with amplitude a sinusoidal function of shaft position. Since the second Hall generator is offset 90^{o} to the first, its output is a cosine function of position. These two signals comprise the resolver output and they are identical in form to those from a wound resolver.

Figure 1A shows the schematic of a wound resolver. The rotor is excited with AC through brushes and slip rings. The stator stack is wound with two output windings, spaced at 90^{o} to each other. By transformer action, through the narrow rotor-to-stator air gap, the two outputs are generated. As the rotor turns, the coupling angles between rotor and stator vary, giving the sine and cosine outputs. It is to be noted that this type of unit will not operate with a "DC Carrier".

Figure 1B shows the schematic of a Hall resolver. Mechanically, the wound rotor, brushes and slip rings are replaced by a cylindrical rotating magnet. The stator and stator windings are replaced by a non-laminated return ring. The Hall voltages are amplified by differential operational amplifiers, since the output of

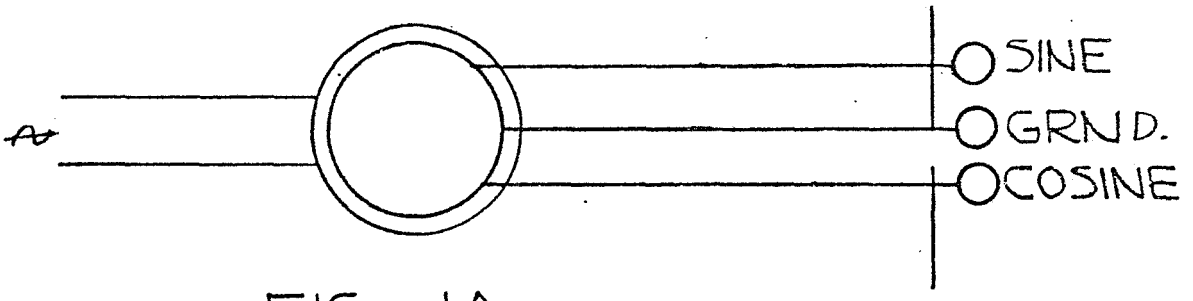
SINE
GRND.
COSINE

FIG 1A

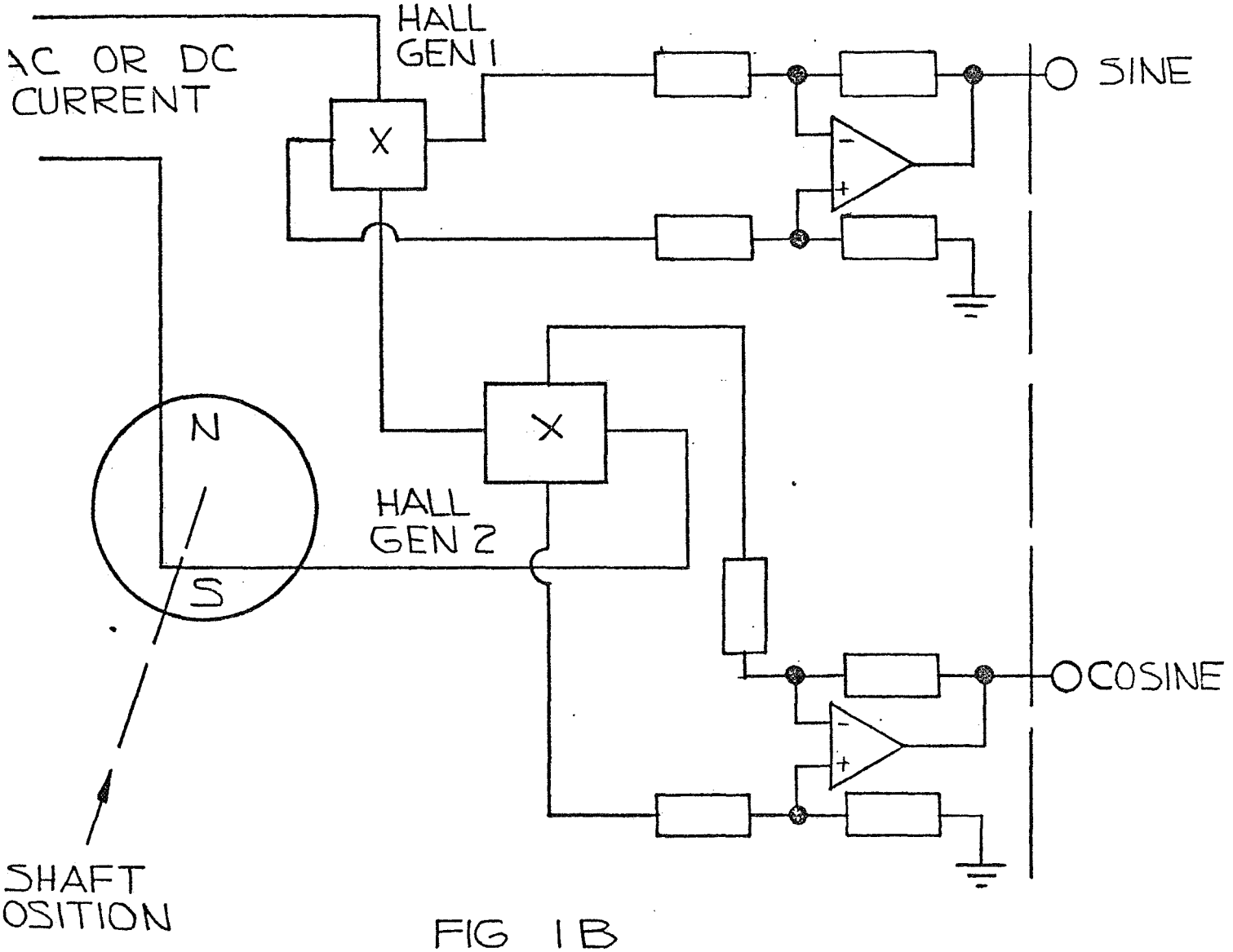
AC OR DC
CURRENT
HALL
GEN 1
X
SINE
N
S
X
HALL
GEN 2
COSINE
SHAFT
OSITION

FIG 1B

Hall generator is a differential voltage, and a single ended output is required. Monolithic integrated circuits may be used to advantage here.

2.0 ERROR ANALYSIS

The general equations of the outputs of the Hall resolver are given in equations 1 and 2 below. Figure 2 shows their graphs.

$$\begin{cases} \text{cosine output} = B = \cos\theta + b_3 \cos 3\theta + b_0 & (1 \\ \text{sine output} = A = K \cos\left(\theta - \frac{\pi}{2} + \alpha\right) \\ \qquad + K\, b_3 \cos\left(3\theta - \frac{3\pi}{2} + 3\alpha\right) & (2 \end{cases}$$

These equations revert to the ideal terms

$$\begin{cases} B = \cos\theta \\ A = \cos\left(\theta - \frac{\pi}{2}\right) \end{cases}$$

$$\text{if} \begin{cases} b_3 = 0 \\ b_0 = 0 \\ K = 1 \\ \alpha = 0 \end{cases}$$

The terms $b_3 \cos 3\theta$ and $Kb_3 \cos(3\theta - \frac{3\pi}{2} + \alpha)$ represents the third harmonic of the spatial flux versus rotation, and are due to imperfections in magnetic imprintation when magnetizing the rotor. No even harmonics will be present as long as the B function possesses even symmetry, and the third will be by far the largest odd harmonic.

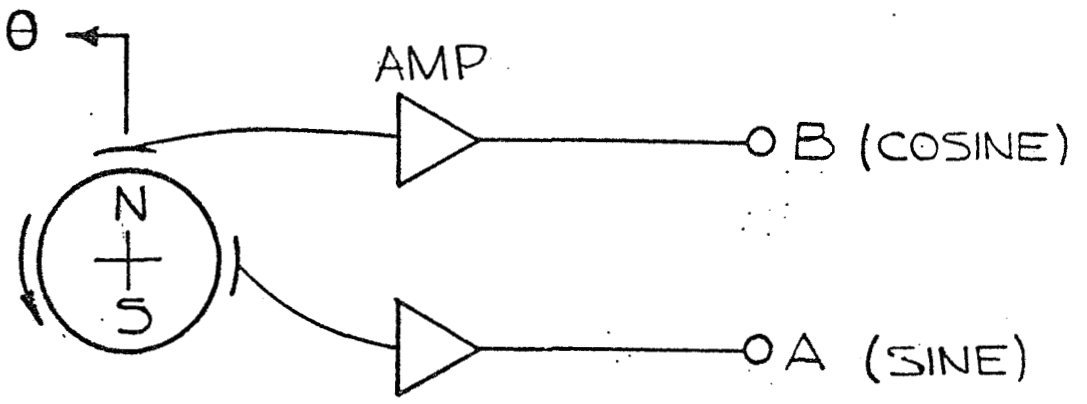
θ
AMP
B (COSINE)
N
S
A (SINE)

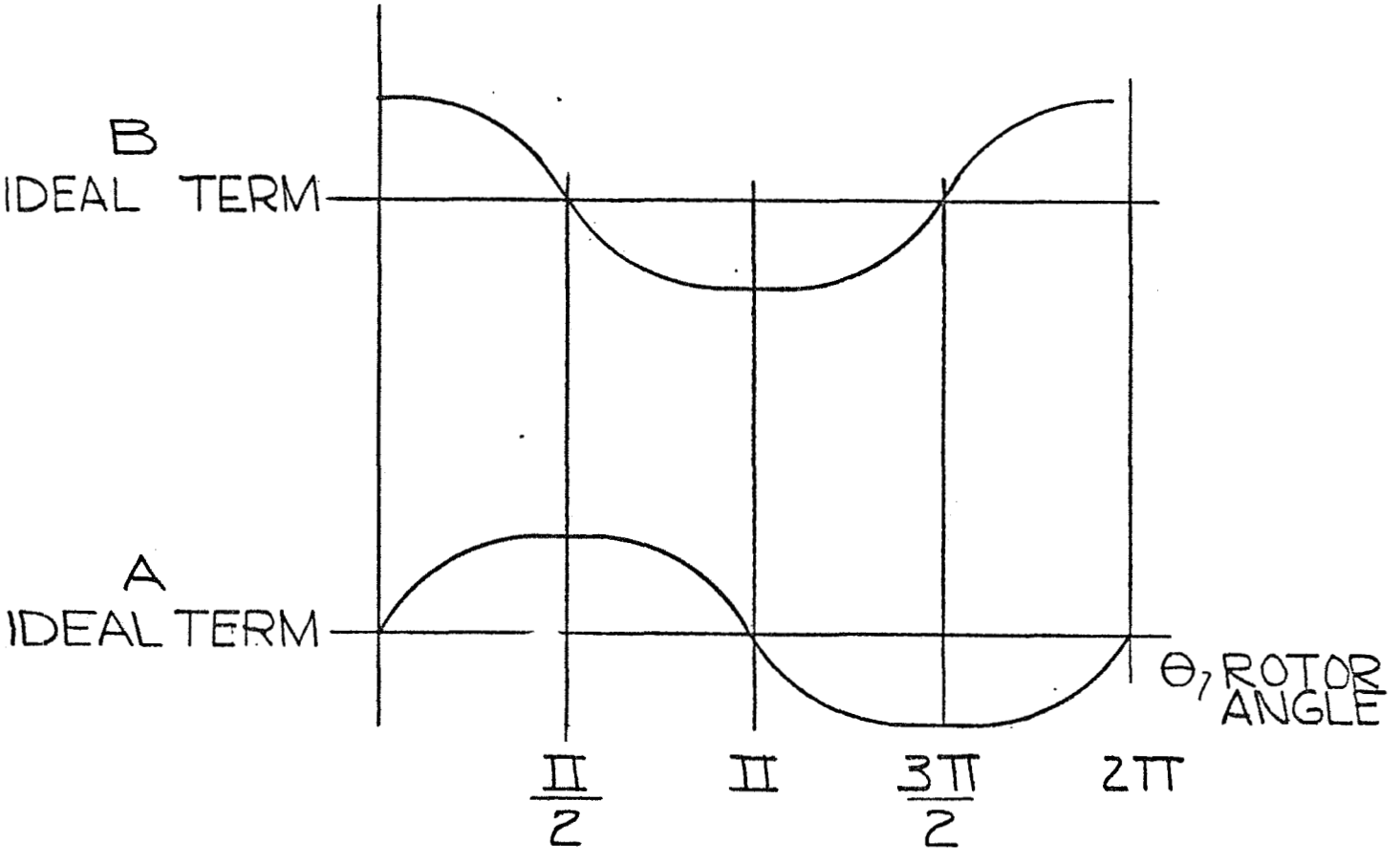
B
IDEAL TERM
A
IDEAL TERM
θ, ROTOR ANGLE
π/2
π
3π/2
2π

FIG 2

The term b_o represents the effect of the finite resistive null of the Hall generators. It may be trimmed to zero at room temperature but in general will drift to some non-zero value.

The coefficient K is the ratio of the transformation ratio of A with respect to B. After initial room temperature adjustment to 1.0, it will drift somewhat due to the lack of tracking of the Hall voltage temperature coefficients with temperature.

The parameter α is the error from perfect perpendicularity of the two Hall generators. It may arise due to relative motions between the Hall generators, caused by temperature coefficients of expansion of the return ring or by self-heating of the Hall generators changing their electrical axis.

2.1 ERROR DUE TO $b_3 \neq 0$ (THIRD HARMONIC FLUX)

In this case $B = \cos \theta + b_3 \cos 3\theta$

$$A = \cos\left(\theta - \frac{\pi}{2}\right) + b_3 \cos\left(3\theta - \frac{3\pi}{2}\right)$$

Figures 3A and 3B show the third harmonic voltages.

$$\theta = \tan^{-1}\left[\frac{\cos\left(\theta - \frac{\pi}{2}\right) + b_3 \cos\left(3\theta - \frac{3\pi}{2}\right)}{\cos\theta + b_3 \cos 3\theta}\right]$$

$$\theta_{ideal} = \tan^{-1}\left[\frac{\cos\left(\theta - \frac{\pi}{2}\right)}{\cos\theta}\right]$$

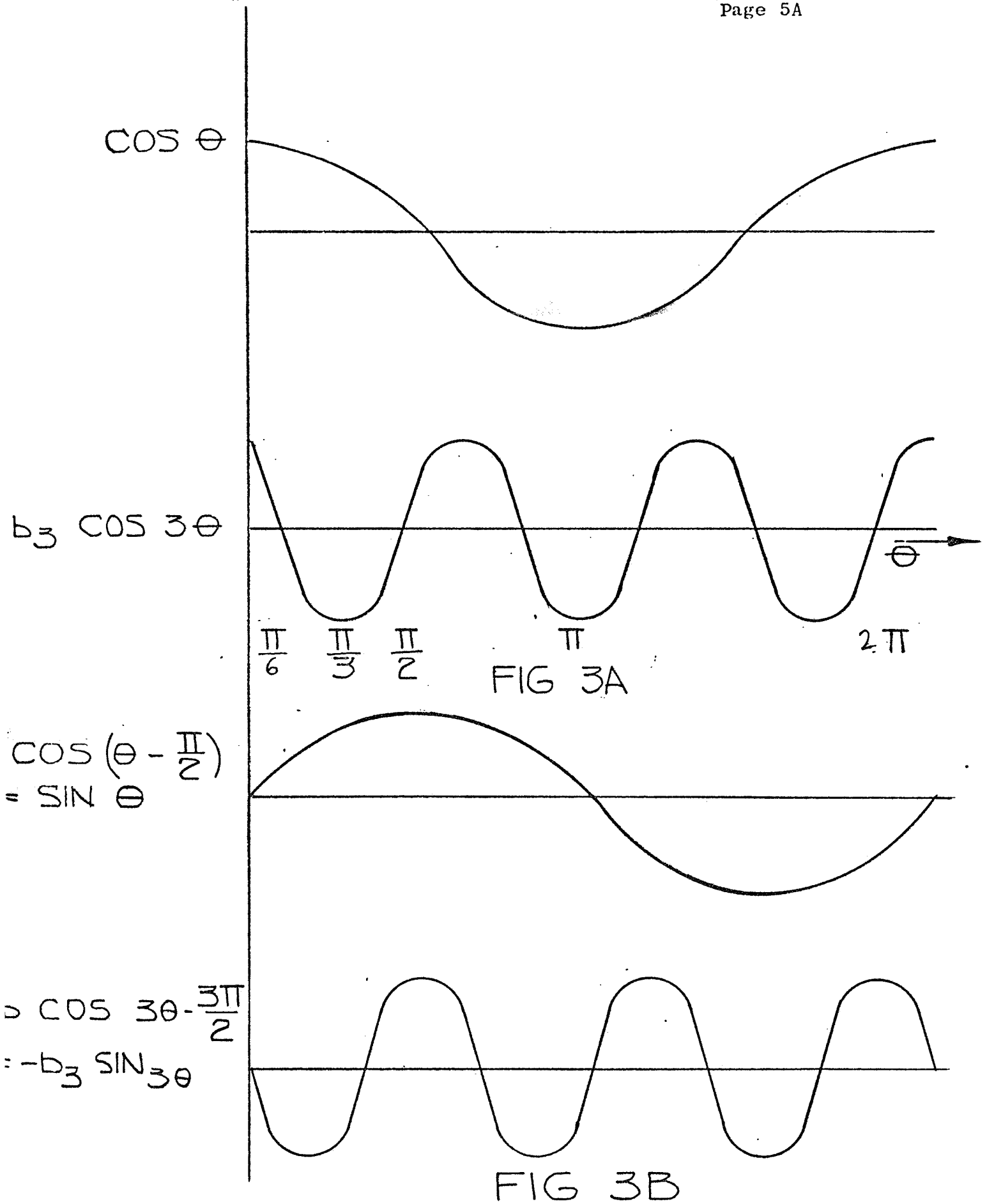

FIG 3A

FIG 3B

$$\Delta\theta = \theta - \theta_{ideal} = \tan^{-1}\left[\frac{\cos\ (\theta - \frac{\pi}{2}) + b_3\ \cos(3\theta - \frac{3\pi}{2})}{\cos\ \theta + b_3\ \cos\ 3\ \theta}\right]$$

$$- \tan^{-1}\left[\frac{\cos\ (\theta - \frac{\pi}{2})}{\cos\ \theta}\right]$$

$$\tan\ \Delta\ \theta = \frac{\left[\frac{\cos(\theta - \frac{\pi}{2}) + b_3\ \cos(3\theta - \frac{3\pi}{2})}{\cos\ \theta + b_3\ \cos\ 3\theta}\right] - \left[\frac{\cos\ (\theta - \frac{\pi}{2})}{\cos\ \theta}\right]}{1 + \left[\frac{\cos(\theta - \frac{\pi}{2}) + b_3\ \cos(3\theta - \frac{3\pi}{2})}{\cos\ \theta + b_3\ \cos\ 3\theta}\right]\left[\frac{\cos(\theta - \frac{\pi}{2})}{\cos\ \theta}\right]}$$

$$= \frac{\left[\cos(\theta - \frac{\pi}{2}) + b_3\ \cos(3\theta - \frac{3\pi}{2})\right]\left[\cos\ \theta\right] - \left[\cos(\theta - \frac{\pi}{2})\right]\left[\cos\theta + b_3\ \cos 3\theta\right]}{(\cos\ \theta + b_3\ \cos 3\theta)\ \cos\theta + \left[\cos(\theta - \frac{\pi}{2}) + b_3\ \cos(3\theta - \frac{3\pi}{2})\right]\left[\cos(\theta - \frac{\pi}{2})\right]}$$

$$= \frac{\cos\theta\left[\cos(\theta - \frac{\pi}{2})\right] + b_3\ \cos\theta\left[\cos(3\theta - \frac{3\pi}{2})\right] - \cos\theta\left[\cos(\theta - \frac{\pi}{2})\right] - b_3\cos 3\theta\left[\cos(\theta - \frac{\pi}{2})\right]}{\cos^2\ \theta + b_3\ \cos\ \theta\left(\cos\ 3\theta\right) + \cos^2(\theta - \frac{\pi}{2}) + b_3\ \cos(\theta - \frac{\pi}{2})\left[\cos(3\theta - \frac{3\pi}{2})\right]}$$

$$= \frac{b_3\left[\cos\theta\left\{\cos(3\theta - \frac{3\pi}{2})\right\} - \cos\ 3\theta\left\{\cos\ (\theta - \frac{\pi}{2})\right\}\right]}{\cos^2\theta + \sin^2\ \theta + b_3\left[\cos\ \theta\left(\cos\ 3\theta\right) + \sin\ \theta\left(\sin\ 3\theta\right)\right]}$$

$$= \frac{b_3\left[-\cos\theta(\sin 3\theta) - \cos 3\theta(\sin\theta)\right]}{1 + b_3\left[\cos\theta(\cos 3\theta) + \sin\theta(\sin 3\theta)\right]} = -b_3\frac{\left[\sin\theta(\cos 3\theta) + \sin 3\theta(\cos\theta)\right]}{1 + b_3\left[\cos\theta(\cos 3\theta) + \sin\theta(\sin 3\theta)\right]}$$

$$= \frac{-b_3 \sin(\theta + 3\theta)}{1 + b_3\left[\cos(\theta - 3\theta)\right]} = \frac{-b_3 \sin 4\theta}{1 + b_3 \cos(-2\theta)}$$

$$\tan\Delta\theta = -b_3 \sin 4\theta \left\{1 - b_3\cos(-2\theta) + \left[b_3\cos(-2\theta)\right]^2 - \ldots\right\}$$

for $b_3 \ll 1$, $b_3\cos(-2\theta) \ll 1$ and may be neglected.

Then since $\Delta\theta$ is small,

$$\Delta\theta \cong \tan\Delta\theta = -b_3 \sin 4\theta$$

2.2 ERROR DUE TO b_0 (RESISTIVE NULL)

In this case,

$$B = \cos\theta + b_o$$

$$A = \cos\left(\theta - \frac{\pi}{2}\right)$$

$$\theta = \tan^{-1}\left[\frac{\cos(\theta - \frac{\pi}{2})}{(\cos\theta) + b_o}\right] = \tan^{-1}\left[\frac{\sin\theta}{(\cos\theta) + b_o}\right]$$

$$\theta_{ideal} = \tan^{-1}\left[\frac{\sin\theta}{\cos\theta}\right]$$

$$\Delta\theta = \theta - \theta_{ideal} = \tan^{-1}\left[\frac{\sin\theta}{(\cos\theta) + b_o}\right] - \tan^{-1}\left[\frac{\sin\theta}{\cos\theta}\right]$$

$$\tan\Delta\theta = \frac{\frac{\sin\theta}{(\cos\theta) + b_o} - \frac{\sin\theta}{\cos\theta}}{1 + \left[\frac{\sin\theta}{(\cos\theta) + b_o}\right]\frac{\sin\theta}{\cos\theta}}$$

$$= \frac{\sin\theta\left(\cos\theta\right) - \sin\theta\left[(\cos\theta) + b_o\right]}{\cos\theta\left[(\cos\theta) + b_o\right] + \sin^2\theta}$$

$$\tan\Delta\theta = \frac{\sin\theta\left(\cos\theta\right) - \sin\theta\left(\cos\theta\right) - b_o\sin\theta}{\cos^2\theta + \sin^2\theta + b_o\cos\theta}$$

$$= \frac{-b_o\sin\theta}{1 + b_o\cos\theta}$$

$$\tan \Delta\theta = -b_o \sin\theta \left[1 - b_o \cos\theta + b_o^2 \cos^2\theta \pm \ldots\right]$$

for $b_o \ll 1$, $b_o \cos\theta$ and higher powers are negligible compared with 1 and since $\Delta\theta$ is small.

$$\Delta\theta = -b_o \sin\theta$$

2.3 ERROR DUE TO $K \neq 1$

In this case

$$B = \cos\theta$$

$$A = K \cos\left(\theta - \frac{\pi}{2}\right) = K \sin\theta$$

$$\theta = \tan^{-1}\left[\frac{K \sin\theta}{\cos\theta}\right]$$

$$\theta_{ideal} = \tan^{-1}\left[\frac{\sin\theta}{\cos\theta}\right]$$

$$\Delta\theta = \theta - \theta_{ideal} = \tan^{-1}\left[\frac{K \sin\theta}{\cos\theta}\right] - \tan^{-1}\left[\frac{\sin\theta}{\cos\theta}\right]$$

$$= \tan^{-1}(K \tan\theta) - \theta$$

$$\tan\Delta\theta = \frac{K\tan\theta - \tan\theta}{1 + K\tan^2\theta} = \frac{\tan\theta\,(K-1)}{1 + K\tan^2\theta}$$

$$\tan\Delta\theta = \frac{\left[(K-1)\tan\theta\right]\left(\frac{\sin^2\theta}{\tan^2\theta}\right)}{\left[1 + K\tan^2\theta\right]\left(\frac{\sin^2\theta}{\tan^2\theta}\right)}$$

$$\tan \Delta\theta = \frac{(K - 1) \sin \theta (\cos \theta)}{\cos^2 \theta + K \sin^2 \theta} = \frac{(K - 1) \sin \theta (\cos \theta)}{\cos^2 \theta + \sin^2 \theta + (K-1) \sin^2 \theta}$$

$$\tan \Delta\theta = \frac{(K - 1) \sin \theta (\cos \theta)}{1 + (K-1) \sin^2 \theta}$$

$$\tan \Delta\theta = (K-1) \sin \theta \cos \theta \left[1 - (K-1) \sin^2\theta + (K-1)^2 \sin^4\theta \pm \ldots\right]$$

For $K \cong 1$, $(K-1) \sin^2\theta$ is negligable compared to 1 and for $\Delta\theta$ small,

$$\Delta\theta = (K-1) \sin \theta (\cos \theta) = (K-1) \frac{\sin 2\theta}{2}$$

2.4 ERROR DUE TO $\neq 0$ (PERPENDICULARITY)

In this case,

$$B = \cos \theta$$
$$A = \cos (\theta - \tfrac{\pi}{2} + \alpha)$$

$$\theta = \tan^{-1}\left[\frac{\cos (\theta - \frac{\pi}{2} + \alpha)}{\cos \theta}\right]$$

$$\theta_{ideal} = \tan^{-1}\left[\frac{\sin \theta}{\cos \theta}\right]$$

$$\Delta\theta = \tan^{-1}\left[\frac{\cos(\theta - \frac{\pi}{2} + \alpha)}{\cos \theta}\right] - \tan^{-1}\left[\frac{\sin \theta}{\cos \theta}\right]$$

$$\tan \Delta\theta = \frac{\frac{\cos(\theta - \frac{\pi}{2} + \alpha)}{\cos \theta} - \frac{\sin \theta}{\cos \theta}}{1 + \left[\frac{\cos(\theta - \frac{\pi}{2} + \alpha)}{\cos \theta}\right]\left[\frac{\sin \theta}{\cos \theta}\right]}$$

$$= \frac{\cos \theta \left[\cos \left(\theta - \frac{\pi}{2} + \alpha\right)\right] - \sin \theta (\cos \theta)}{\cos^2 \theta + \sin \theta \cos \left(\theta - \frac{\pi}{2} + \alpha\right)}$$

$$\tan \Delta\theta = \frac{\cos \theta \left[\sin \theta (\cos \alpha) + \cos \theta \sin \alpha\right] - \sin \theta (\cos \theta)}{\cos^2 \theta + \sin \theta \left[\sin \theta (\cos \alpha) + \cos \theta (\sin \alpha)\right]}$$

$$\tan \Delta\theta = \frac{\cos \theta (\sin \theta)(\cos \alpha) + \cos^2 \theta (\sin \alpha) - \sin \theta (\cos \theta)}{\cos^2 \theta + \sin^2 \theta (\cos \alpha) + \sin \theta (\cos \theta)(\sin \alpha)}$$

$$\tan \Delta\theta = \frac{\cos \theta (\sin \theta)(\cos \alpha - 1) + \cos^2 \theta (\sin \alpha)}{\cos^2 \theta + \sin^2 \theta + (\cos \alpha - 1) \sin^2 \theta + \sin \theta \cos \theta \sin}$$

$$\tan \Delta\theta = \frac{\cos \theta \left[\sin \theta (\cos \alpha - 1) + \cos \theta (\sin \alpha)\right]}{1 + \sin \theta \left[\sin \theta (\cos \alpha - 1) + \cos \theta (\sin \alpha)\right]}$$

For α small, $\sin \theta \left[\cos \alpha - 1\right] + \cos \theta (\sin \alpha)$ is negligable compared to 1.

$$\tan \Delta\theta = \cos \theta \left[\sin \theta (\cos \alpha - 1) + \cos \theta \sin \alpha\right]$$

For α small, $\cos (\alpha - 1)$ is much smaller than $\sin \alpha$, and will be neglected in comparison, and also for small $\Delta\theta$,

$$\Delta\theta \cong \tan \Delta\theta = \cos^2 \theta (\sin \alpha) = \alpha \cos^2 \theta$$

3.0 SUMMARY

Table 1 summarizes the errors.

3.1 THIRD HARMONIC MAGNET FLUX

It is seen that a third harmonic magnet flux gives rise to a fourth harmonic analog error. The peak magnitude is b_3 radians where b_3 is the amplitude of the 3rd harmonic flux. The fourth harmonic has peaks at $\frac{\pi}{8}$ and $\frac{3\pi}{8}$, and is zero at 0, $\frac{\pi}{4}$, and $\frac{\pi}{2}$. Physically at $\frac{\pi}{4}$ both sine and cosine outputs have distortion, but are equal, giving no error. Multispeeding reduces errors due to this source. However, if multispeeding increases the 3rd harmonic distortion as it might due to the crowding effect of poles on a limited amount of circumference, the net effect of multispeeding might not increase with n, or might even decrease.

3.2 RESISTIVE NULL ERROR

This gives an electrical fundamental error of magnitude b_o, where b_o is the resistive null relative to 1. The error phase is determined by the channel which has the resistive null. This error reduces by n in a multispeed system.

3.3 GAIN UNBALANCE ERROR

The result of a gain unbalance is a 2nd electrical harmonic output. The phase of this is such that the error is zero at 0, $\frac{\pi}{2}$, π, etc and peaks at $\frac{\pi}{4}$, $\frac{3\pi}{4}$, etc. This is under-

standable since when either the sine or cosine is zero, there can be no error due to gain unbalance. Multi-speeding reduces this error source.

3.4 NON-PERPENDICULARITY ERROR

The result of an error in mechanical placement between the Hall sensors is seen as a $\cos^2$ or double frequency error with a DC bias. This undirectional error has magnitude of α degrees. The phase of this error curve is at quadrature to the gain unbalance error above. This error may be considered to be halved and be an error of $+\frac{\alpha}{2}$, and $-\frac{\alpha}{2}$ merely by using a new angle reference point for 0°.

Multispeeding does not influence the magnitude of this error.

ERROR CAUSE	RESULTANT RESOLVER ERROR	
	SINGLE SPEED	n-SPEED
THIRD HARMONIC MAGNET FLUX OF AMPLITUDE b_3	$-b_3 \sin 4\theta$	$\frac{1}{n}(-b_3 \sin 4\theta)$
RESISTIVE NULL VOLTAGE b_o	$-b_o \sin \theta$	$\frac{1}{n}(-b_o \sin \theta)$
GAIN UNBALANCE ERROR, GAIN RATIO K	$\left[\frac{K-1}{2}\right] \sin 2\theta$	$\frac{1}{n}\left(\left[\frac{K-1}{2}\right] \sin 2\theta\right)$
NON-PERPENDICULAR PLACEMENT ERROR	$\alpha \cos^2 \theta$	$\alpha \cos^2 \theta$

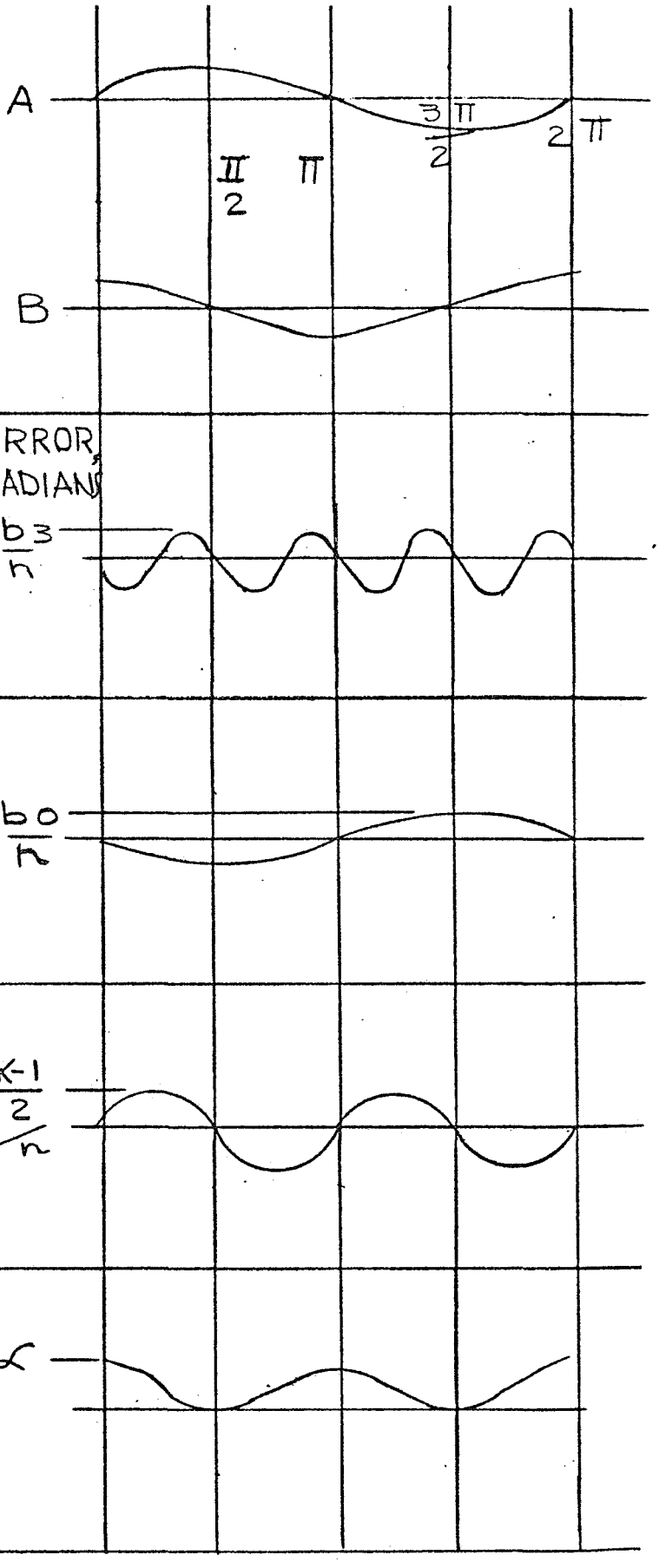

TABLE I. ERROR CONTRIBUTIONS

To: Engineering File MT-14,609

From: H. Swanson

Issue: Original

Date: 11/10/69

HALL RESOLVER TEST REPORT

Prepared by: H. Swanson
H. Swanson

Approved by: M. DeMeo
M. DeMeo

THE BENDIX CORPORATION
NAVIGATION AND CONTROL DIVISION
TETERBORO, NEW JERSEY

1.0 INTRODUCTION

This report contains test results and analysis of a D. C. Mounted Torquer and associated electronics (General Electric Drawing No. 852D360) that has been modified as described below to allow testing of the Hall Generator sections of the assembly as a resolver.

The two existing Hall generators on the GFE torquer were excited with a 1000 Hz input voltage. The two Hall voltage outputs were amplified and were then compatible with a laboratory resolver bridge.

The Hall driver amplifier, Hall compensation network, and Hall summing amplifiers of the GFE electronics were used and were modified for AC operation by using a 1000 Hz signal source as input to the Hall driver. The amplitude was adjusted for approximately 25 ma peak Hall control current which is the rated control current for operation in air for the SV110 Type III, Hall generator.

The modifications to the summing amplifiers were to disconnect their outputs from the rest of the torquer electronics, addition of feedback resistors to give a stable lower gain necessitating a change in the R-C stabilizing components for the lower gain connection.

Figure 1 shows the circuitry with the modifications, additional components added, and circuit paths opened. The modifications include the addition of four feedbacks

16.2 K resistors, opening the feedback branch of the 24.9 K Ω resistor and 0.027 uf capacitor in series, and using the compensation capacitors called for in the non-current feedback connection of the torquer.

With these modifications, the outputs were 1.9 V peak for each section at maximum coupling.

2.0 ELECTRICAL CHARACTERISTICS

The measured electrical characteristics of the Hall Resolver are as listed below. A discussion of the results follows in Section 3.0.

Number of Poles	6
Input Voltage (Volts Peak)	0.44
Frequency (Hz)	1000
Accuracy (Electrical Degrees)	+7.13/-2.17
Nulls (mv. max.)	
Total	2.6
Fundamental	0.7
Sine Deviation (%RMS)	
Sine Output	1.425
Cosine Output	1.35
Transformation Ratio	
Sine Output	4.21
Cosine Output	4.18
Phase Shift (degrees)	-2.88
Accuracy vs. Voltage (electrical degrees)	0.102

3.0 DISCUSSION OF TEST RESULTS

3.1 Analog Accuracy

The Hall generator was excited with 0.44 volts peak 1000 Hz signal as shown in Figure 1. As the shaft is rotated thru 360°, the flux pattern of the 6 pole permanent magnet rotor develop 6 pole voltage output at each Hall generator. These Hall devices being physically displaced 90° from each other develop the 3 speed sine and cosine resolver outputs that vary in magnitude with position of the shaft.

The analog or tangent function accuracy is obtained by comparison of the sine and cosine outputs using the test circuit shown in Figure 5. The test results are plotted in Figure 2.

A Fourier analysis of the error pattern, shown in Table I, shows that the 12th, 6th, and 1st error harmonics, given in order of magnitude of error, contribute most significantly to the total error. These are space harmonics of which the 3rd space harmonic is the fundamental electrical signal harmonic. Therefore, the error harmonics relative to the electrical fundamental are, in order of magnitude of error, the 4, 2, and 1/3 harmonics. The magnitudes shown in Table I are in electrical degrees of error, therefore, by dividing each error by three (electrical fund.) the mechanical shaft position error is obtained.

The 1st space harmonic error is 0.8341 electrical degrees or 0.278 mechanical degrees. This space harmonic error is attributed to the fact that there is an accumulation of eccentricities between mechanical shaft center of rotation and the magnetic center of rotation. Also an eccentricity between the unit mechanical center and the indexing head center.

To give more insight to the cause of the remaining major error harmonics, the outputs of both the sine and cosine channels were measured and a Fourier Analysis (See Tables II and III) was performed.

The test circuit used to measure both channel outputs is shown in Figure 6 and the plot of the test data is given in Figures 3 and 4. To eliminate error due to line voltage variation, the output was measured as a ratio of the input by using a Hewlett Packard 3450A Rotiometer.

The similarity of both the sine and cosine Fourier Analysis shows there is no detectable distortion contributed by the Hall sensors; therefore, it is an MMF wave distortion attributed to the permanent magnets. The third MMF space harmonic is the signal MMF wave (Electrical Fundamental) and all the other harmonics are distortions which contribute to the unit error (see MT-14,620, Sources of Hall Resolver Errors).

The 12th space harmonic error is attributed to the 9th and 15th space MMF harmonics. From Table II we obtain:

$$D_9 = \text{Distortion 9th MMF} = \frac{E_9}{E_3} = \frac{.1910}{4.1149} = .0465$$

$$D_{15} = \text{Distortion 15th MMF} = \frac{E_{15}}{E_3} = \frac{.0204}{4.1149} = .0049$$

The magnitude of 12th harmonic error attributed to this distortion is as follows:

$$RU_{12\ \text{error}} = D_9 \times 57.3 \text{ degrees/radion}$$
$$= .0465 \times 57.3 = 2.62 \text{ elect. degree}$$

$$RU_{12\ \text{error}} = D_{15} \times 57.3 = .0049 \times 37.3$$
$$= 0.28 \text{ elect. degrees}$$

The total 12th harmonic error is the summation of error due to the 9th and 15th MMF harmonic distortions. Therefore, we obtain 2.9 electrical degrees which compares with the 2.95 electrical degree 12th harmonic error measured (see Table I). This 12th space harmonic error is the 4th electrical harmonic error described in MT-14,620.

In Table I we also see a 6th space harmonic error which is the 2nd electrical harmonic error described in MT-14,620. From that report it is shown that the 2nd electrical harmonic error is due to gain unbalance between the sine and cosine channels and a perpendicularity error between the peak outputs of each channel. From Table II and Table III we see:

RU_S = Sine Channel Output = $4.115 \angle 1.51^\circ$

RU_C = Cosine Channel Output = $4.061 \angle 93.24^\circ$

From the report we see that the gain unbalance error is:

$$BU_6 \text{ error} = \frac{RU_S - RU_C}{2\,RU_S} \times 57.3 \text{ elect. degrees}$$

$$= \frac{4.115 - 4.061}{2\,(4.115)} \times 57.3 = 0.373 \text{ elect. degrees}$$

The perpendicularity error is the amount the sine channel output angle differs from the cosine channel angle (see MT-14,620); therefore, we obtain:

$$AU_6 \text{ error} = \frac{(\angle RU_C - \angle RU_S) - 90}{2} =$$

$$= \frac{93.24 - 1.51 - 90}{2} = 0.865^\circ$$

Table I shows that BU_6 was 0.461 as compared to 0.373 calculated and AU_6 was 0.737° as compared to 0.869° calculated.

3.2 Analog Accuracy vs. Voltage

In order to determine the effect a change in excitation might have on the analog accuracy, the unit was checked at three discrete points with a $\pm$ 15% change of input

to the Hall generator. The maximum deviation in accuracy at any one point was 0.102 electrical degrees. This change represents approximately 1% increase in error.

ANGLE	INPUT VOLTAGE (Volts Pk.)	ERROR (Electrical Degrees)	Δ
	0.44	0	-
180°	0.37	.027	+.027
	0.50	-.046	-.046
	0.44	-2.064	-
174	0.37	-2.016	+.048
	0.50	-2.166	-.102
	0.44	-1.774	-
172	0.37	-1.700	+.074
	0.50	1.864	-.090

ANALOG ACCURACY VS. INPUT VOLTAGE

With the unit at 172°, the input voltage was increased to 0.52 volts peak where saturation of the Hall generator occurred. The analog accuracy at this point was now -1.984 electrical degrees which was a change of 0.210 electrical degrees from normal excitation.

3 Transformation Ratio And Phase Shift

Figure 7 shows the test circuit used to measure the transformation ratio and phase shift of both sine and cosine outputs. The ratio of three maximum sine output was 4.18 with a phase shift of -2.88° and there was a 0.24% maximum variation between the three ratios. The

three cosine output ratios measured were 4.21 with a phase shift of -2.88° and balanced within 0.71%.

3.4 Nulls

The total and fundamental null voltages were measured using the same test circuit as was used to check the analog accuracy. The maximum total null was 2.6 mv and while the maximum fundamental null was 0.7 mv, converting to mv null/output we have:

$$\frac{\text{mv}}{\text{volt}} = \frac{\text{NULL MEASURED}}{(\text{Input Pk.})\ (.707)\ (\text{T.R.})}$$

$$\text{Total} = \frac{2.6 \times 10^{-3}\ \text{mv}}{(0.44\ \text{volts Pk.})\ (.707)\ (4.18)} = 2.0\ \text{mv/volt out}$$

$$\text{Fundamental} = \frac{0.7}{(0.44\ \text{volts Pk.})\ (.707)\ (4.18)} = 0.54\ \text{mv/volt out.}$$

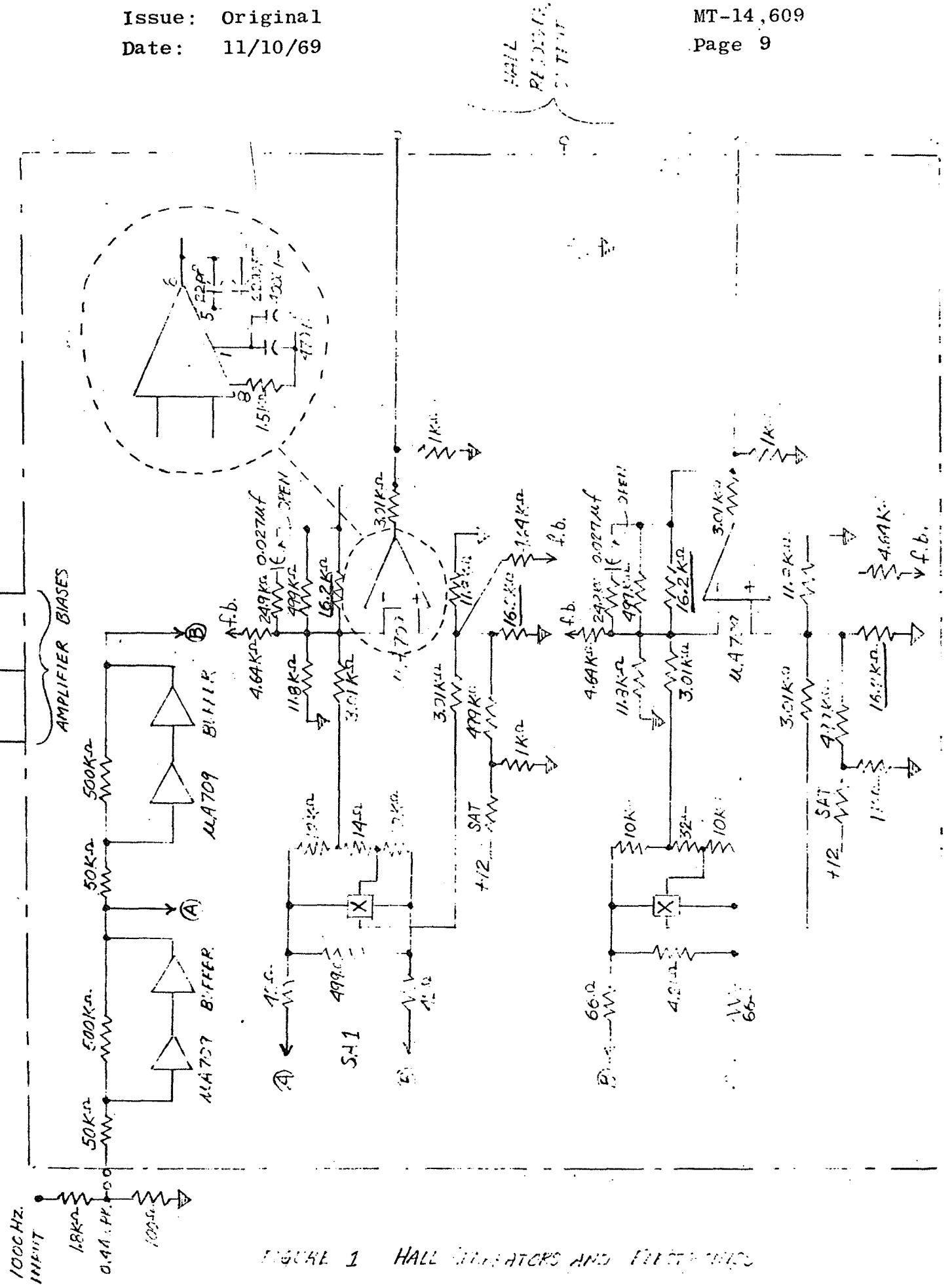

FIGURE 1 HALL GENERATORS AND PREAMPS

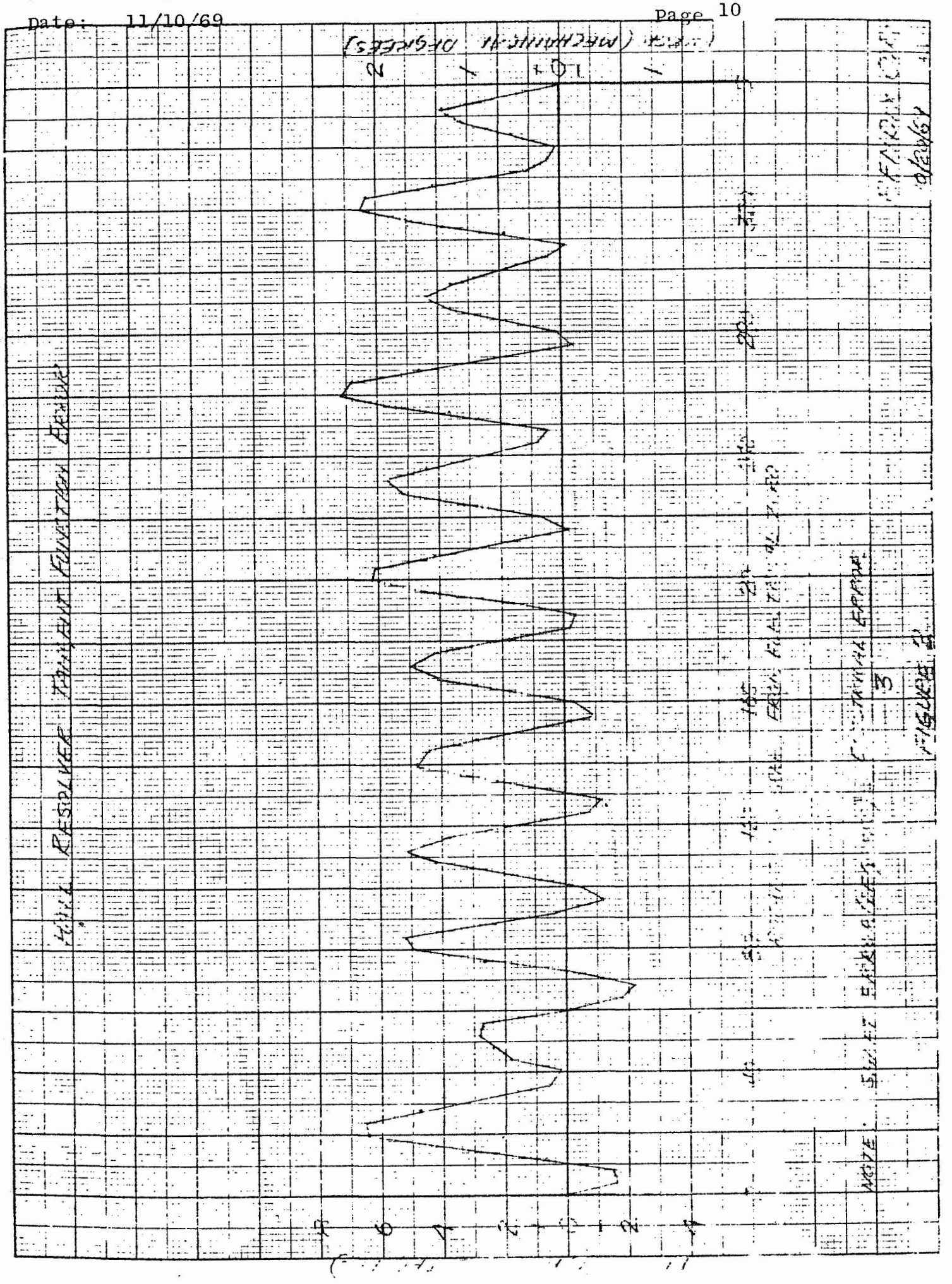

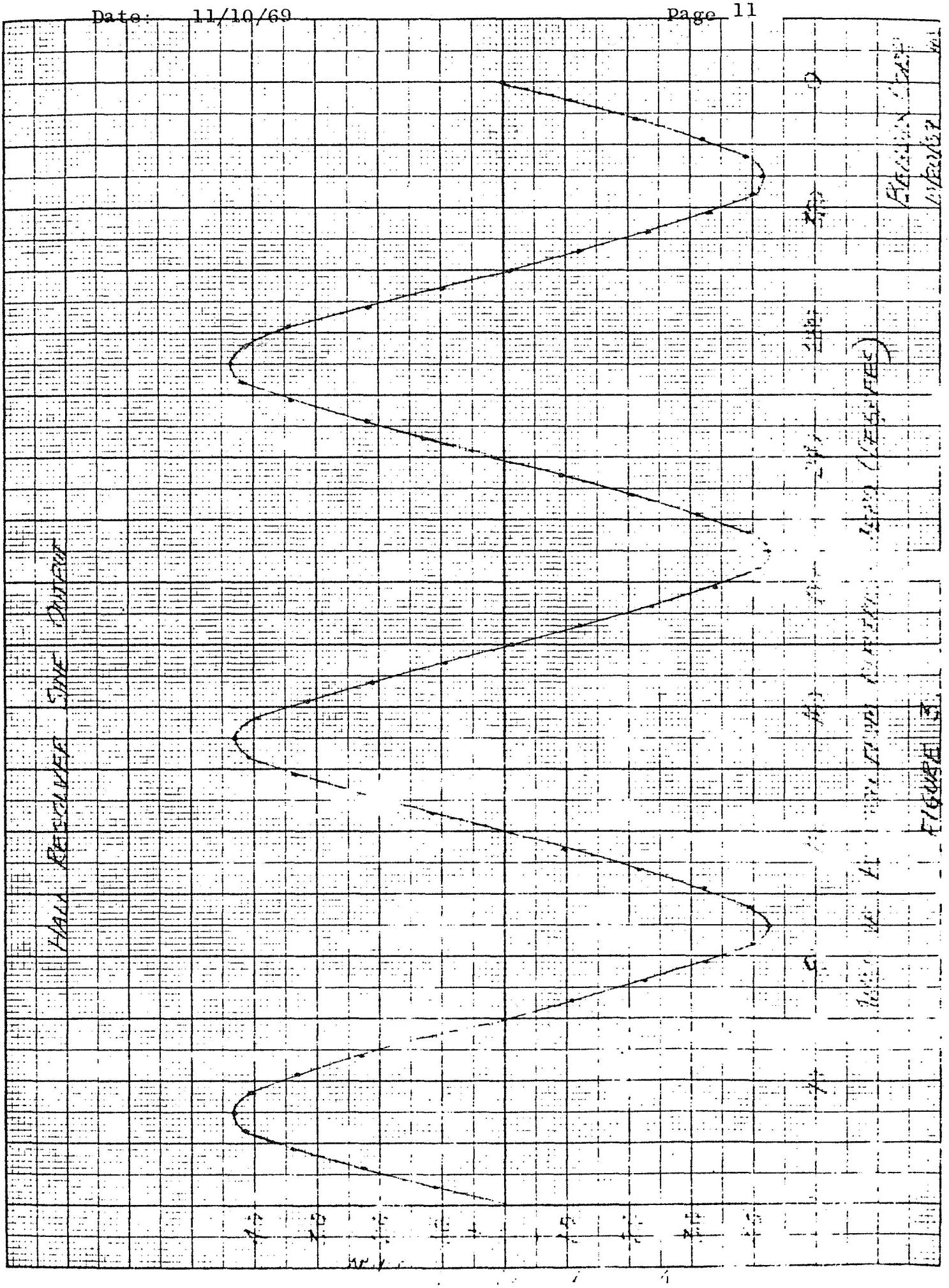

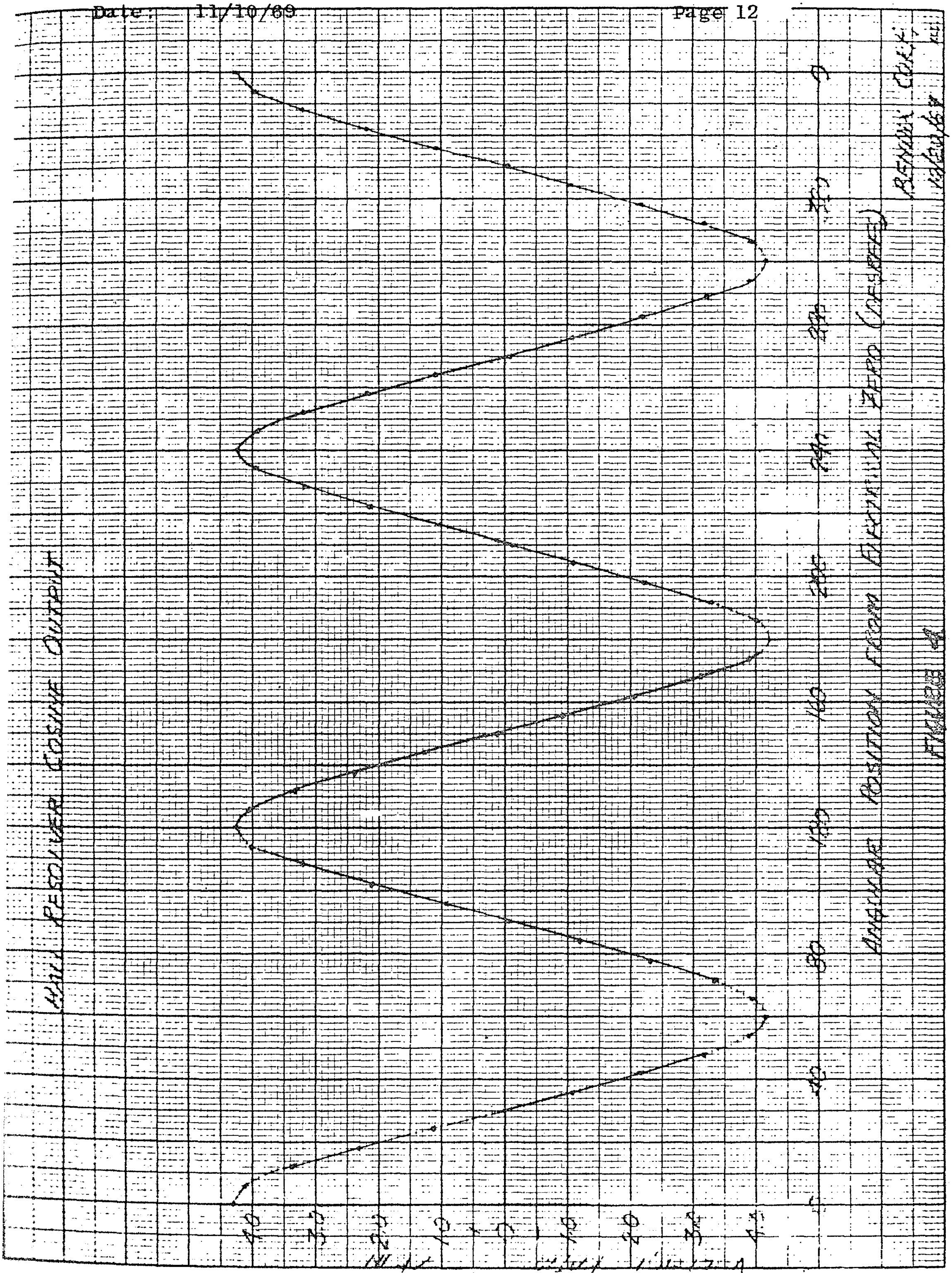
HALL RESOLVER COSINE OUTPUT
ANGULAR POSITION FROM ELECTRICAL ZERO (DEGREES)

FIGURE 4

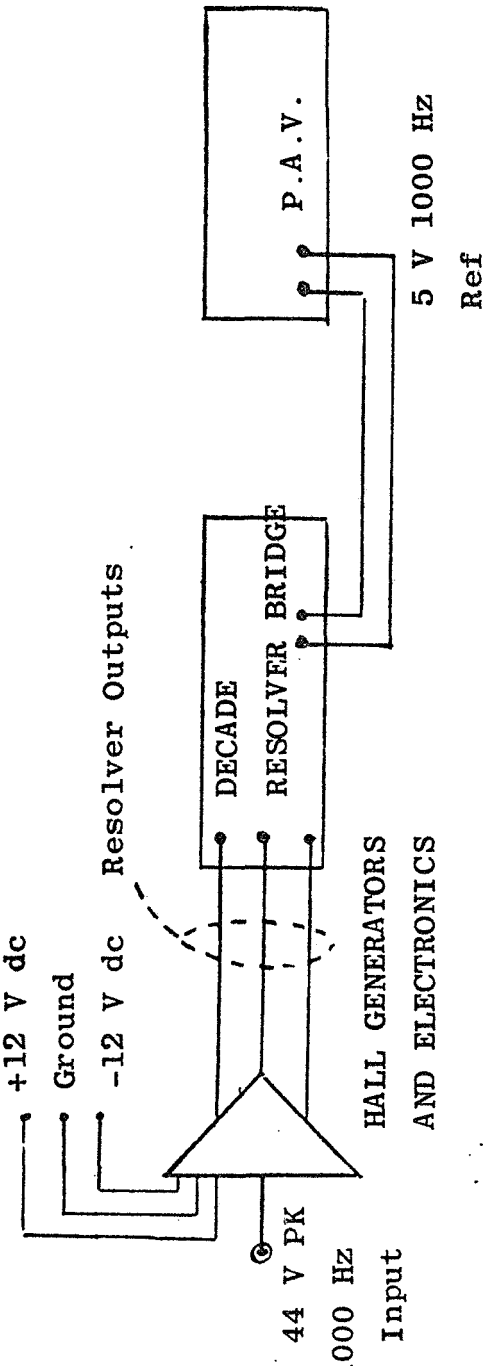

FIGURE 5 - ANALOG ACCURACY

Test Equipment

Gertsch Decade Resolver Bridge D5RB-4R

Gertsch P.A.V. Model 2AR

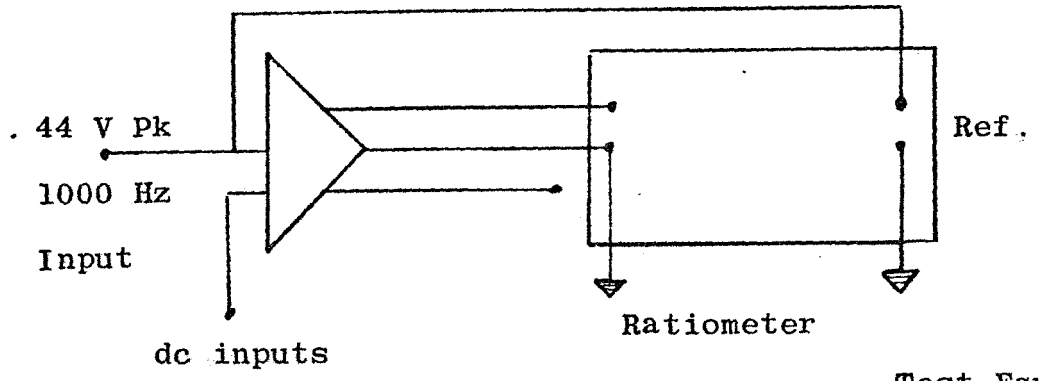

Test Equipment

Hewlett Packard 3450A Ratiometer

FIGURE 6 - SINE DEVIATION

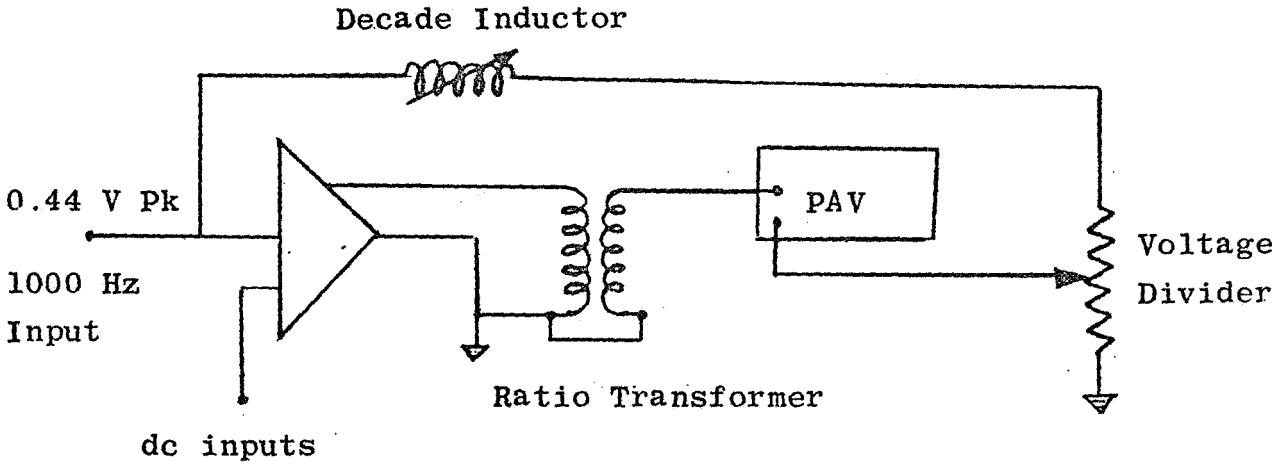

Test Equipment

Gertsch Ratio Transformer Model 10
General Radio Decade Inductor
Type No. 940E
General Radio Voltage Divider
Type No. 1454
Gertsch P.A.V. Model 2AR.

FIGURE 7 - TRANSFORMATION RATIO

ANALOG ACCURACY FOURIER ANALYSIS

SPACE HARMONIC U	BU	AU	RU	PHASE
1.0	-0.8055	-0.2165	0.8341	-164.9
2.0	0.1009	0.0163	0.1022	9.1
3.0	0.0316	0.1798	0.1825	80.0
4.0	0.2251	-0.1702	0.2822	-37.0
5.0	0.1751	-0.6783	0.7005	-75.5
6.0	0.4612	-0.7368	0.8692	-57.9
7.0	0.0938	-0.1996	0.2205	-64.8
8.0	-0.2121	-0.1839	0.2808	-139.0
9.0	-0.1826	-0.0725	0.1965	-158.3
10.0	0.0404	-0.0075	0.0411	-10.5
11.0	0.0412	0.0501	0.0648	50.5
12.0	-2.9103	-0.4909	2.9514	-170.4
13.0	0.1055	0.0522	0.1177	26.3
15.0	-0.0073	-0.0856	0.0859	-94.8
18.0	-0.0242	0.0708	0.0749	108.8
24.0	0.0751	0.0673	0.1008	41.9

TABLE I

$$\text{Total Error} = \sum_{0}^{U} AU \cos U\theta + BU \sin U\theta$$

$$= \sum_{0}^{U} RU \sin (U\theta + \angle U)$$

AU, BU, RU are error magnitudes given in electrical degrees.

SINE OUTPUT FOURIER ANALYSIS (MMF PATTERN)

HARMONIC U	BU	AU	RU	PHASE
1.0	0.0007	0.0116	0.0116	86.7
2.0	0.0477	-0.0385	0.0613	-38.8
3.0	4.1135	0.1084	4.1149	1.5
4.0	-0.0236	-0.0279	0.0366	-130.2
5.0	-0.0161	-0.0056	0.0170	-160.7
6.0	-0.0065	-0.0273	0.0281	-103.4
7.0	0.0136	-0.0195	0.0238	-55.0
8.0	0.0092	-0.0030	0.0097	-18.0
9.0	-0.1904	-0.0152	0.1910	175.4
10.0	0.0034	0.0025	0.0042	36.6
11.0	-0.0022	-0.0091	0.0093	-103.3
12.0	-0.0101	0.0027	0.0104	165.0
13.0	-0.0044	0.0028	0.0052	147.4
14.0	-0.0055	0.0030	0.0063	151.5
15.0	-0.0202	-0.0029	0.0204	171.9

TABLE II

$$\text{Total Ratio} = \sum_{0}^{U} AU \cos\theta + BU \sin\theta = \sum_{0}^{U} RU \sin(U\theta + \underline{U})$$